

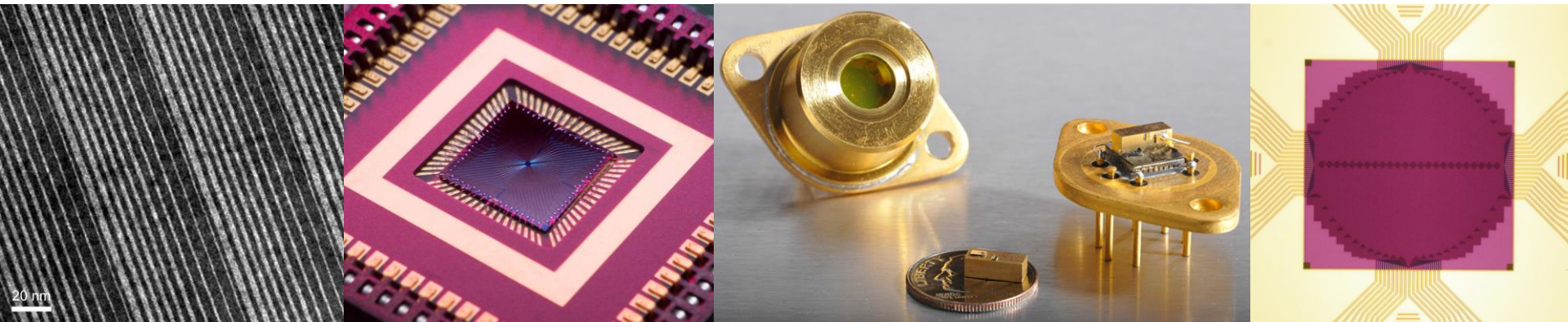
# Infrared Sources and Detectors for Deep-Space Science

Ryan M. Briggs

*Jet Propulsion Laboratory, California Institute of Technology  
Pasadena, California, USA*

*IEEE Metropolitan Los Angeles Section Meeting*

August 3, 2017



Jet Propulsion Laboratory  
California Institute of Technology

---

# Acknowledgements

## **QC Lasers:**

### **- Coworkers:**

Clifford Frez, Mathieu Fradet, Mahmood Bagheri, Siamak Forouhar, and Chris Webster, *JPL*  
Christian Pflügl, Romain Blanchard, and Laurent Diehl, *Pendar Technologies*

### **- Project support:**

NASA Planetary Instrument Concepts and Solar System Observations (PICASSO) Program  
NASA New Frontiers Homesteader Program

## **SNSPDs:**

### **- Coworkers:**

Matthew Shaw, Andrew Beyer, Francesco Marsili, Jason Allmaras, and Bill Farr, *JPL*

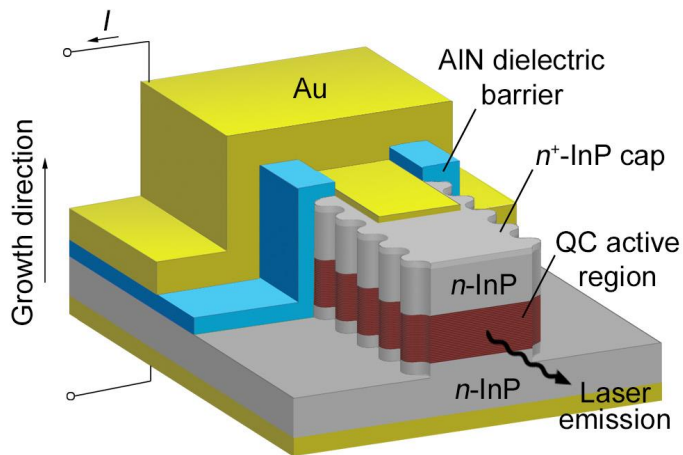
### **- Project support:**

NASA Game Changing Development Program  
JPL Research And Technology Development Program

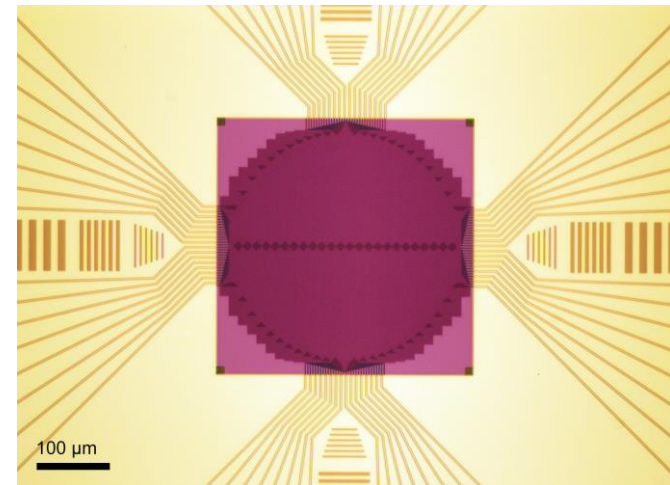


# Overview

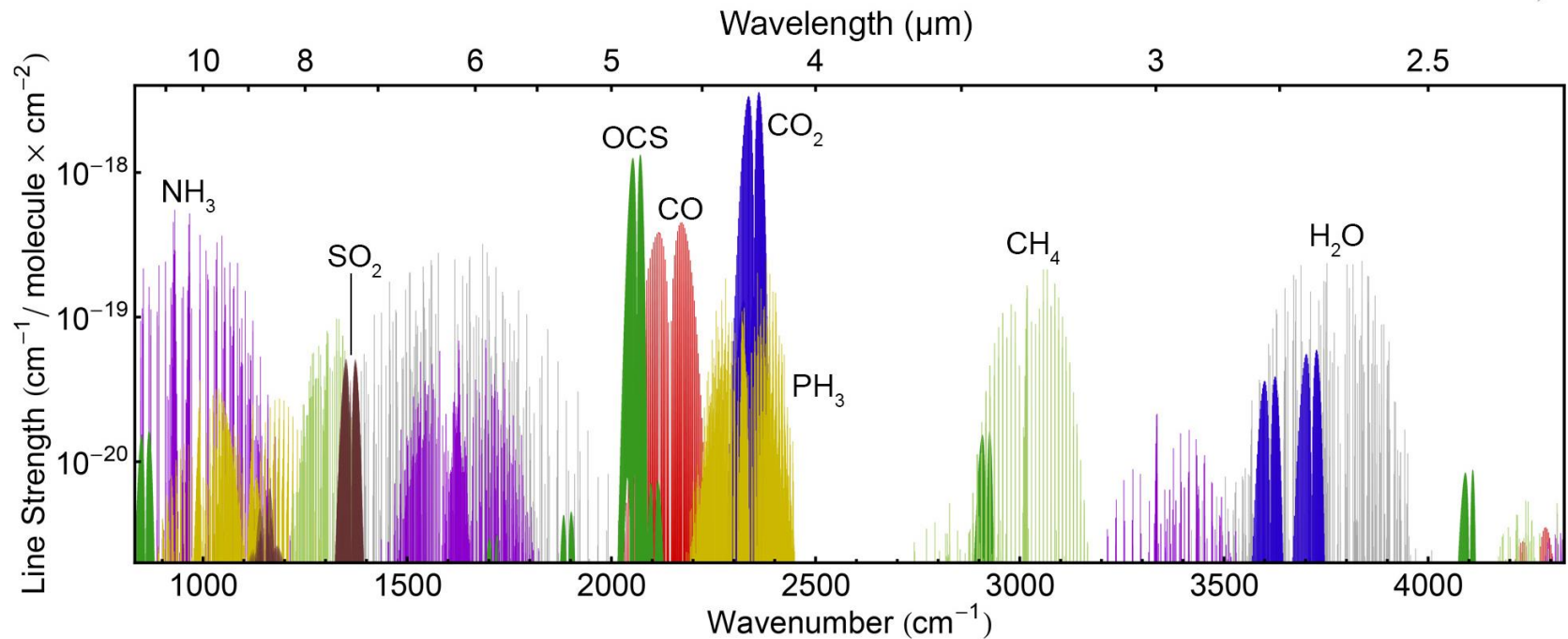
Low-power consumption quantum cascade (QC) lasers for *in situ* gas absorption spectroscopy



Superconducting nanowire single-photon detector (SNSPD) arrays for deep space optical communication

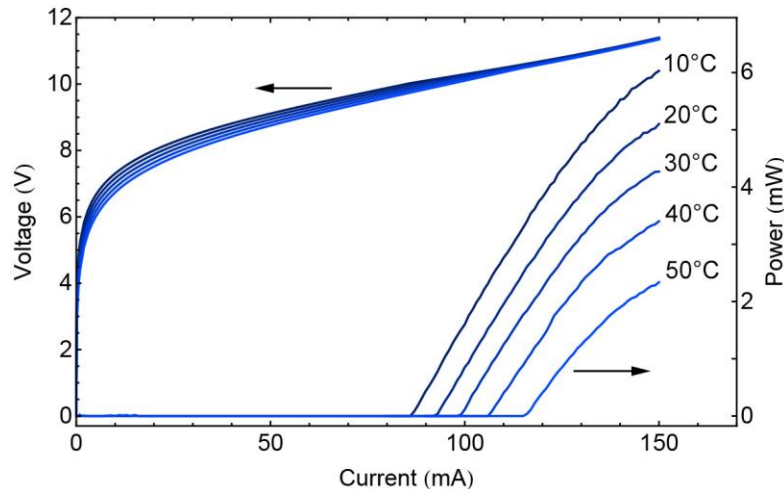


## Molecular absorption in the mid-infrared regime

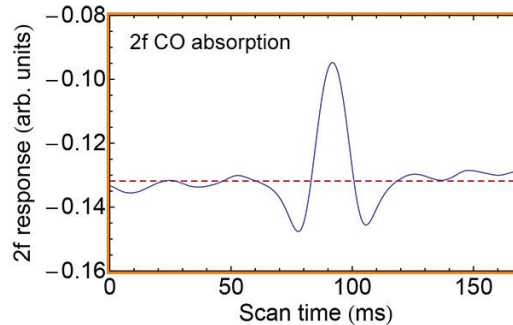
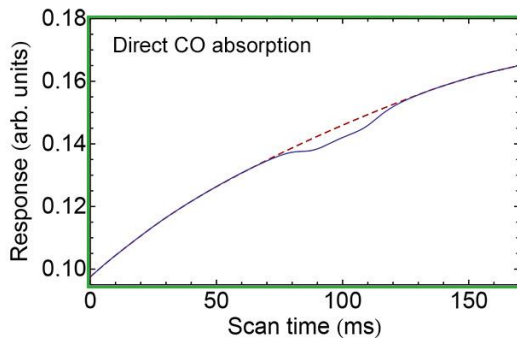


# Laser wavelength modulation spectroscopy

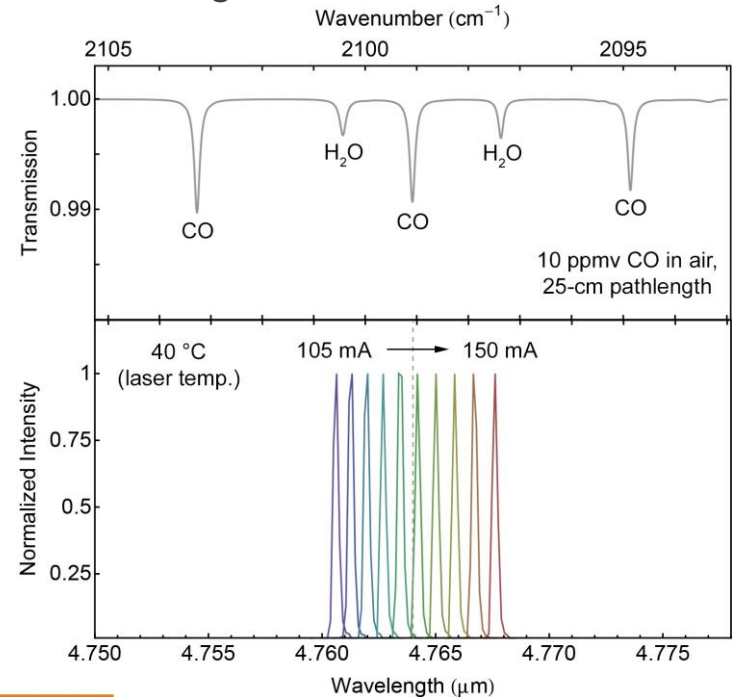
## Laser light-current-voltage characteristics



By sweeping current sourced to a single-mode laser, relative absorption is measured over a known pathlength



## Current tuning of laser emission wavelength



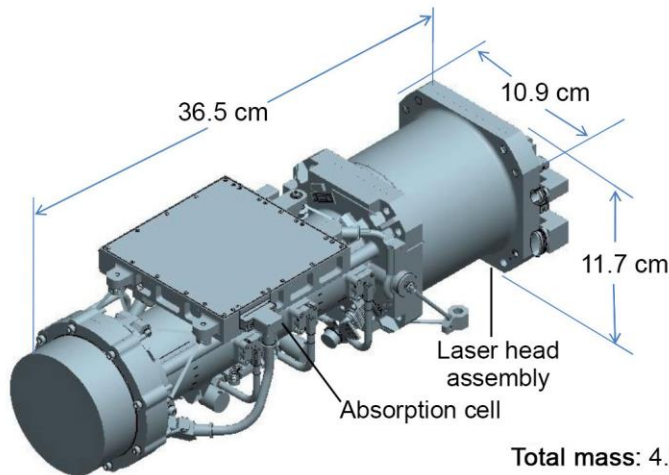
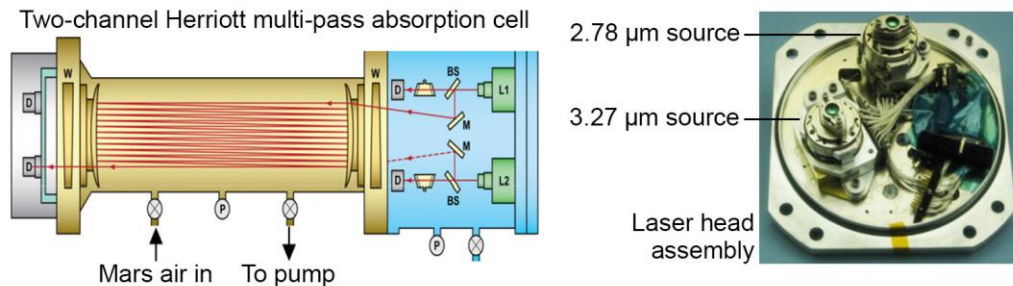
With additional small-amplitude modulation of the current, the demodulated spectral response can be measured with reduced noise





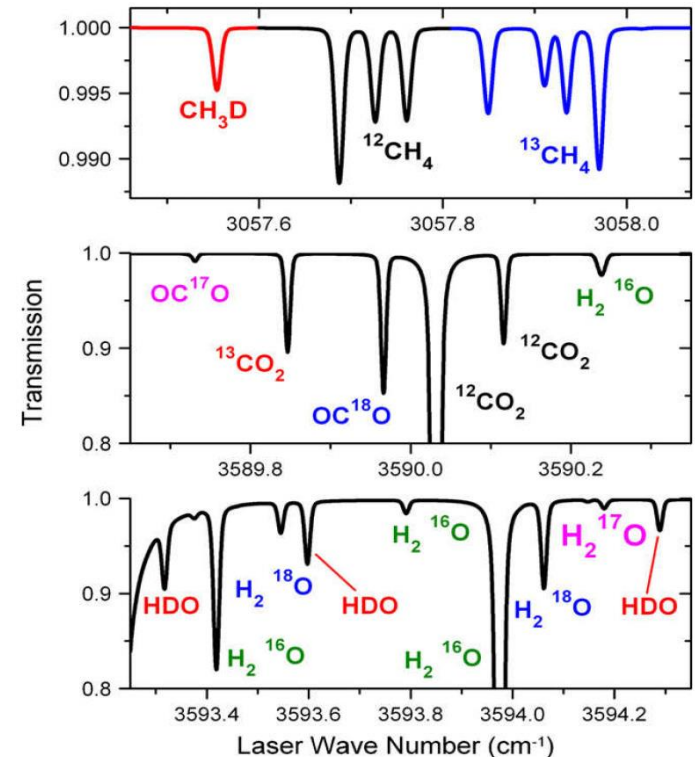
# Tunable Laser Spectrometer (TLS) on the Mars Curiosity rover

## TLS instrument layout for $\text{CH}_4$ and $\text{CO}_2/\text{H}_2\text{O}$ detection



Total mass: 4.5 kg  
Input power: 25 W (16.7 W avg.) @ 28 V  
Operating temperature: -20 to +40 °C  
Survival temperature: -40 to +100 °C

## Target absorption lines



Webster, *et al.*, *Science* **341**, 260 (2013)  
Webster, *et al.*, *Science* **347**, 415 (2015)



Jet Propulsion Laboratory  
California Institute of Technology

# Tunable Laser Spectrometer (TLS) on the Mars Curiosity rover

## C, O, and H isotope ratios in Martian atmosphere

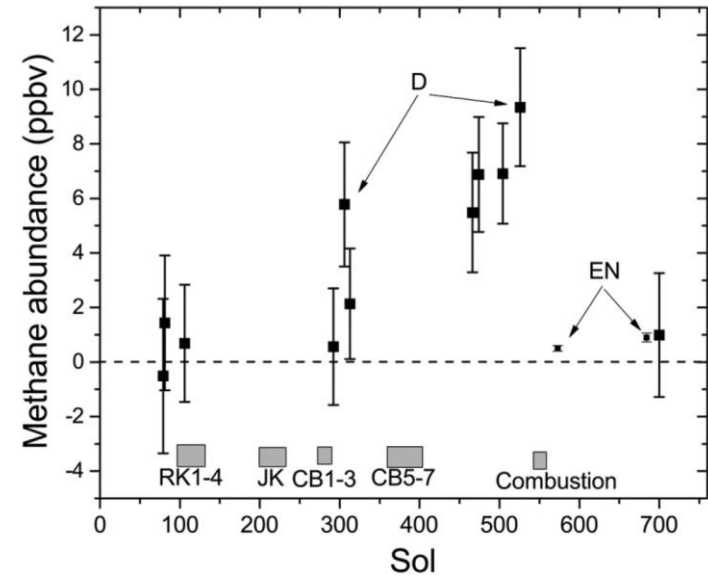
**Table 1. Carbon dioxide isotope ratios ‰ ± 2 SEM (standard error of the mean). \***, not measured.

| Measurement                                   | $\delta^{13}\text{C}$ | $\delta^{18}\text{O}$ | $\delta^{17}\text{O}$   | $\delta^{13}\text{C}^{18}\text{O}$ |
|---|-----------------------|-----------------------|---|------------------------------------|
| SAM-TLS                                       | 46 ± 4                | 48 ± 5                | 24 ± 5  | 109 ± 31                           |
| SAM-QMS (3)                                   | 45 ± 12               | *                     | *   | *                                  |
| Phoenix lander (12)                           | -2.5 ± 4.3            | 31.0 ± 5.7            | *   | *                                  |
| Viking Neutral Mass Spectrometer (11)         | 23 ± 43               | 7 ± 44                | *   | *                                  |
| SNC meteorites (8, 12, 32)                    | 36 ± 10               | 3.9–5.4 ± 0.1         | ~0.53* $\delta^{18}\text{O} \sim \delta^{13}\text{C} + \delta^{18}\text{O}$ |                                    |
| ALH84001 meteoritic carbonate range (30, 31)  | 27 to 64              | -9 to 26              | ~0.53* $\delta^{18}\text{O} \sim \delta^{13}\text{C} + \delta^{18}\text{O}$ |                                    |
| ALH84001 meteoritic carbonate mean value (31) | 46 ± 8                | 4.6 ± 1.2             | *   | *                                  |
| Earth telescopes (9)                          | -22 ± 21              | 18 ± 18               | *   | *                                  |

**Table 2. Water isotope ratios ‰ ± 2 SEM. \***, not measured.

| Measurement  | $\delta\text{D}$ | $\delta^{18}\text{O}$ |
|--|------------------|-----------------------|
| SAM-TLS atmosphere                                       | 4950 ± 1,080     | *                     |
| SAM-TLS evolved water: Rocknest fines 230° to 430°C (23) | 5880 ± 60        | 84 ± 10               |
| Meteoritic crustal reservoirs (26)                       | ~5000            | *                     |
| Earth telescopes (24)                                    | 1700–8900        | *                     |
| ALH 84001 (17)   | 3000             | *                     |
| Shergotty USNM 321-1 (17)                                | 4600             | *                     |

## Methane abundance on Mars



Webster, et al., *Science* **341**, 260 (2013)

Webster, et al., *Science* **347**, 415 (2015)



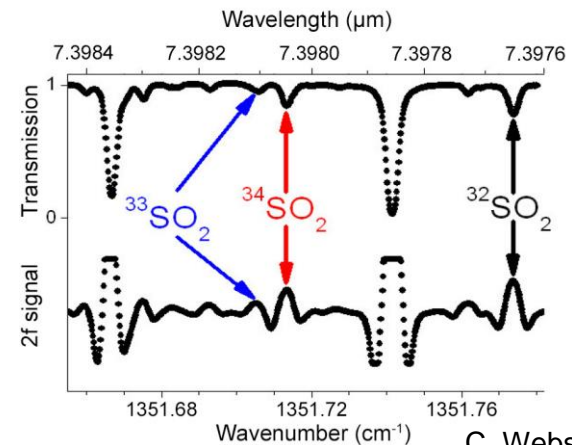
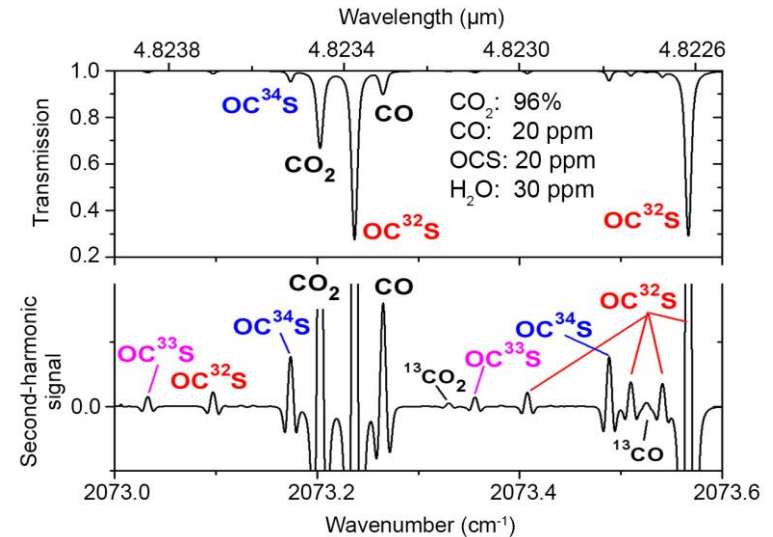
# Future planetary science instruments: Venus In Situ Explorer

## Venus In Situ Explorer atmospheric probe concept



NASA

## Target molecules: OCS and SO<sub>2</sub>



C. Webster, JPL

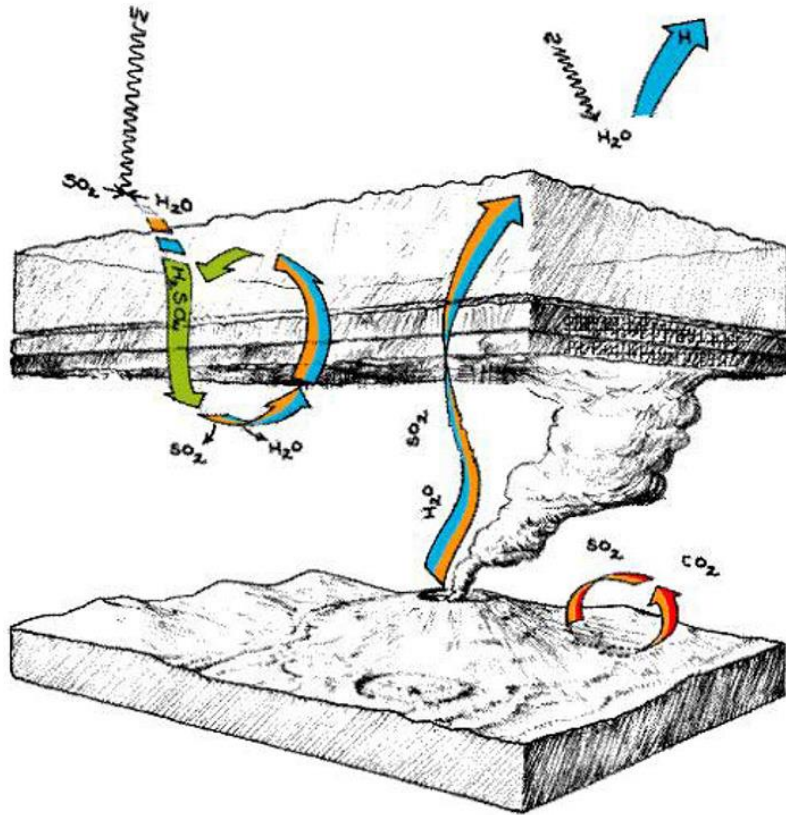


Jet Propulsion Laboratory  
California Institute of Technology



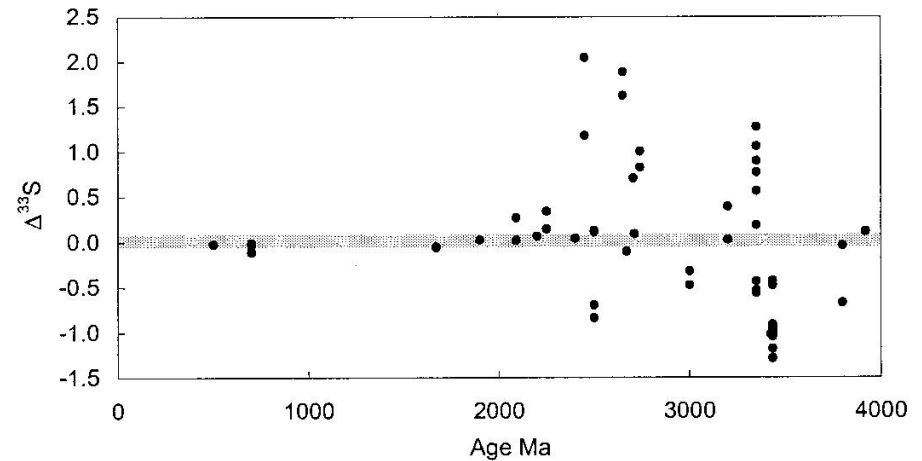
# Future planetary science instruments: Venus In Situ Explorer

## Photolysis and the sulfur cycle on Venus



D. Grinspoon and C. Emmart, NASA

## Geological sulfur isotope record on Earth



Farquhar, *et al.*, Science **289**, 756 (2000)

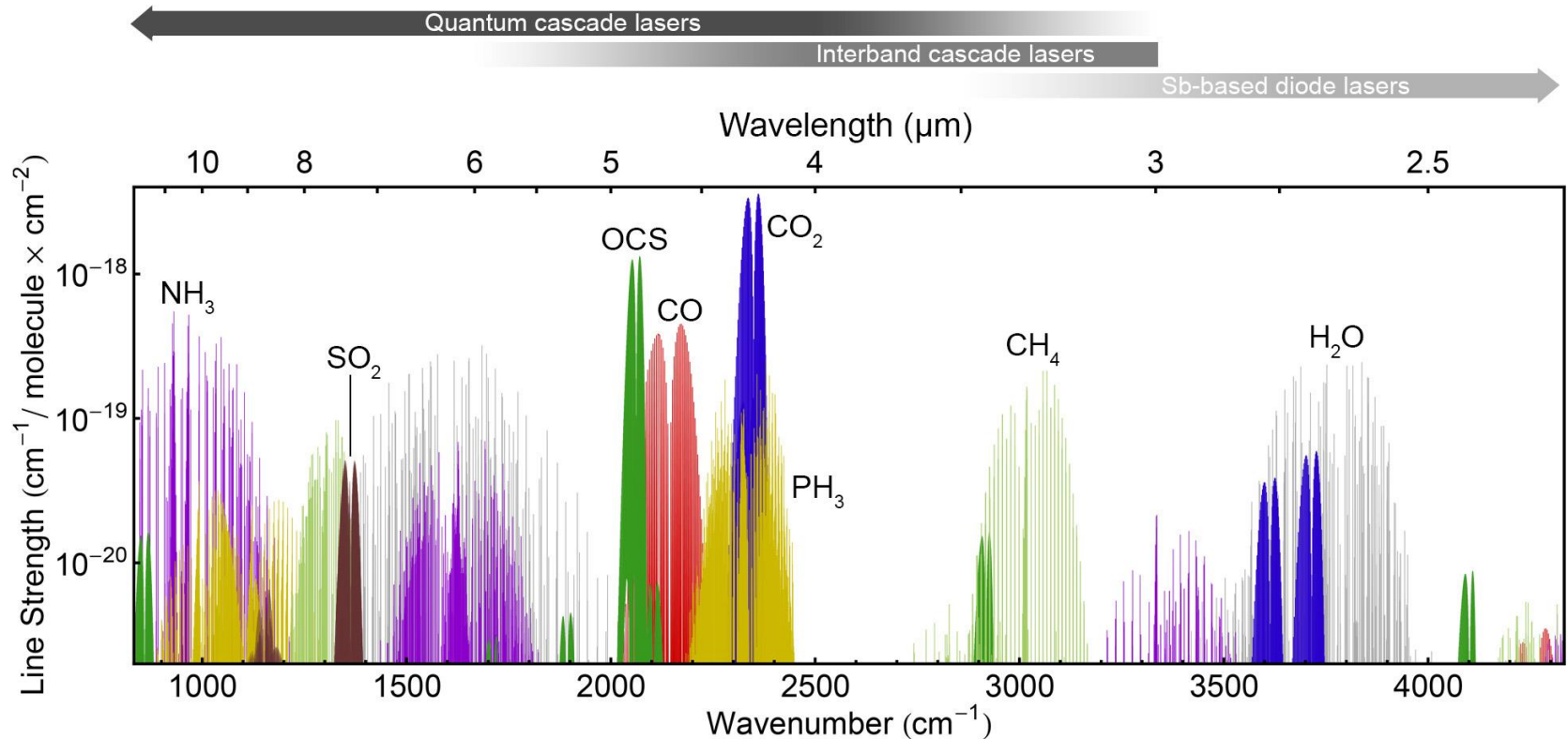
S isotope measurements are a primary objective for proposed missions to Venus

Isotope ratios are key to understanding climate cycles on Venus and can verify theories of the evolution of Earth's atmosphere



Jet Propulsion Laboratory  
California Institute of Technology

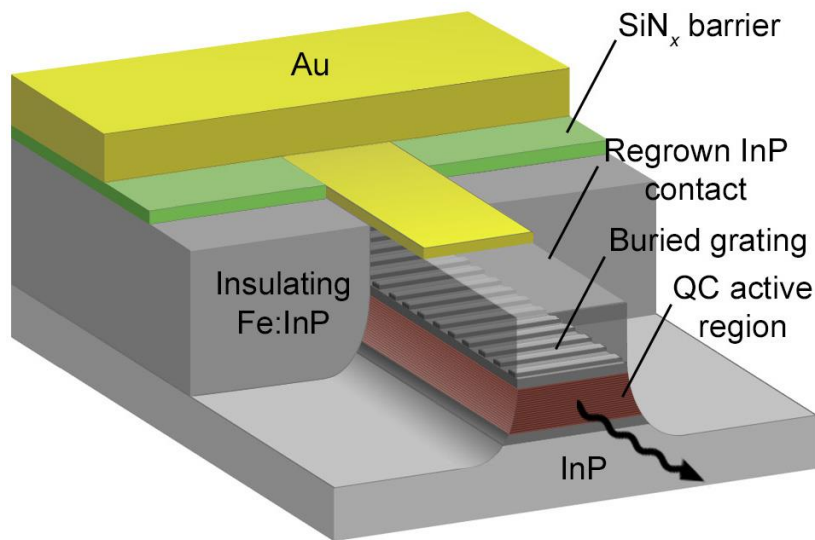
# Semiconductor laser technologies for TLS instruments



Future laser spectrometers will target longer-wavelength lines, which will require QC lasers  
Power consumption is a limiting factor in component selection



# Buried-heterostructure DFB QC lasers

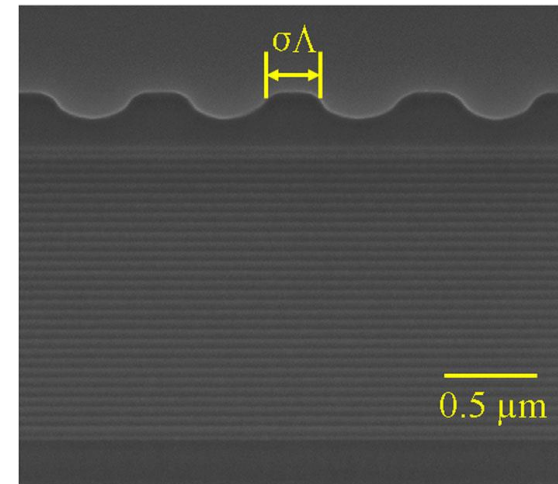


Provides low optical loss, excellent heat dissipation, and reliability, but requires two epitaxial regrowth processes

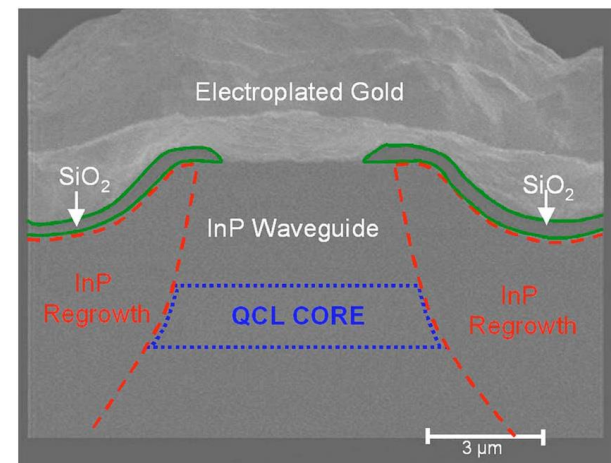
Mid-infrared emission with sub-watt power consumption recently demonstrated by ETH Zürich and Alpes Lasers

Hinkov, et al., *Electron. Lett.* **646**, 071101 (2012)

Bismuto, et al., *Opt. Express* **23**, 5477 (2015)



Zhang, et al., *Appl. Phys. Lett.* **100**, 112105 (2012)

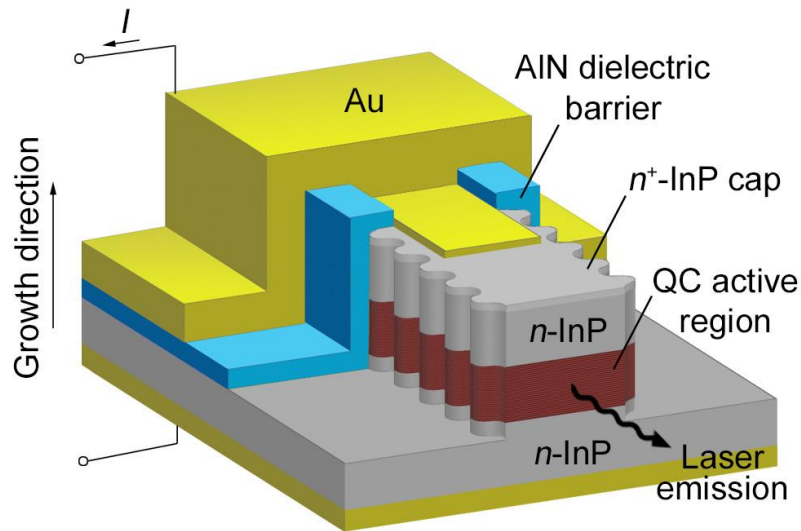


Evans, et al., *Appl. Phys. Lett.* **91**, 071101 (2007)



Jet Propulsion Laboratory  
California Institute of Technology

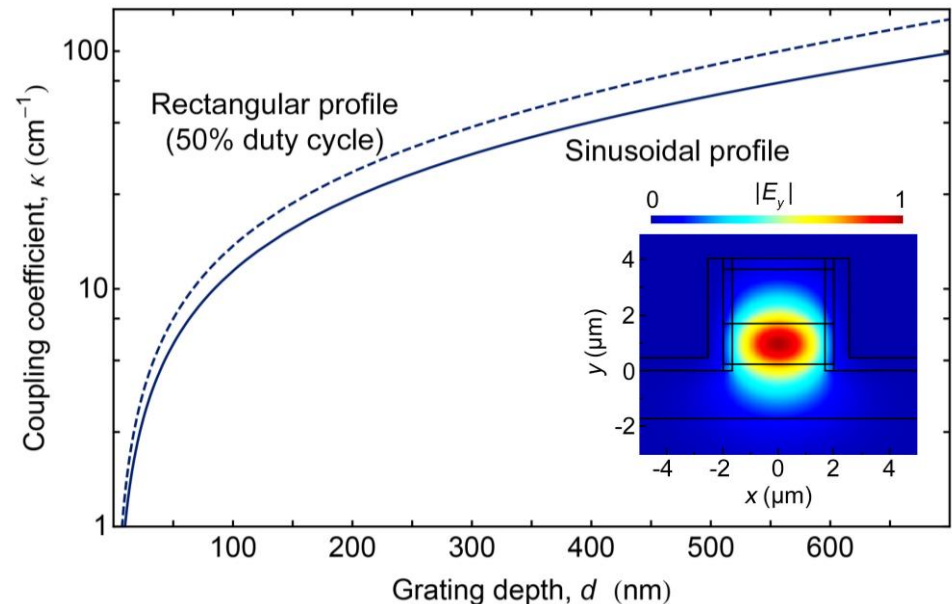
# Regrowth-free DFB QC laser design



Sidewall gratings with low-index dielectric cladding provide high optical confinement

Narrow, vertically etched ridges enable low-current operation

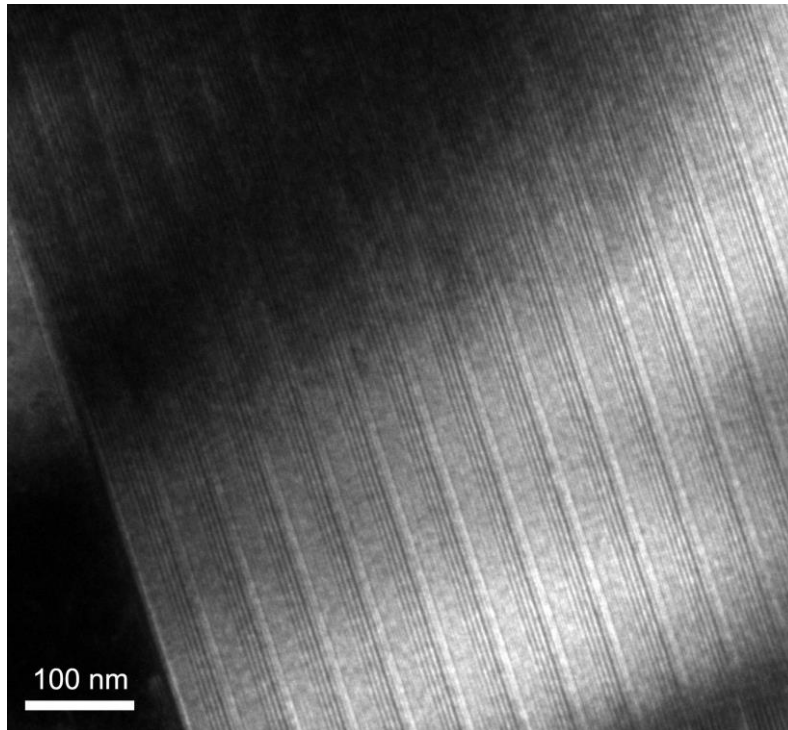
Calculated grating coupling coefficient:  
4.8  $\mu\text{m}$  wavelength, 775 nm pitch





# Fabrication of DFB QC lasers

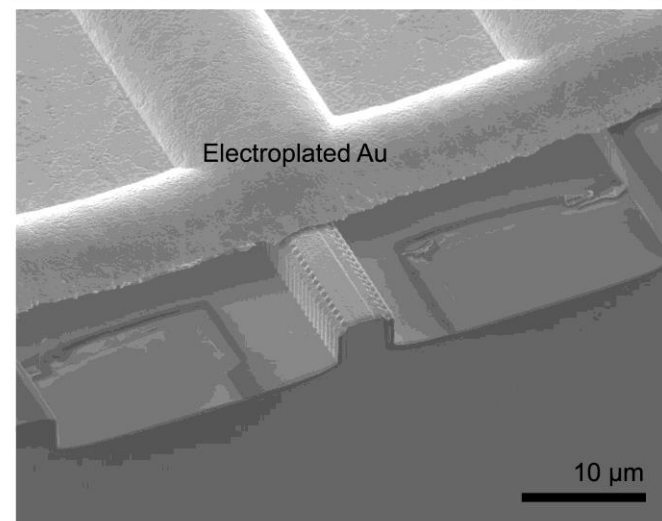
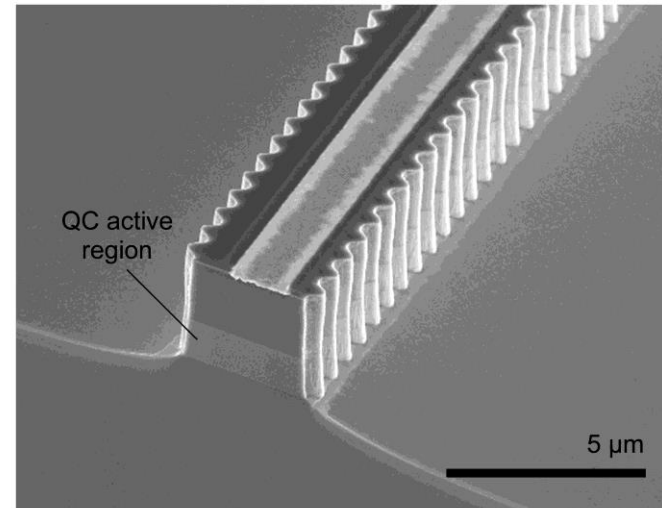
MBE-grown QC active region on InP



Transmission electron microscopy by M. Sullivan (Caltech)

Two-phonon-resonance design used  $<5 \mu\text{m}$ ,  
non-resonant extraction designs employed  $>5 \mu\text{m}$

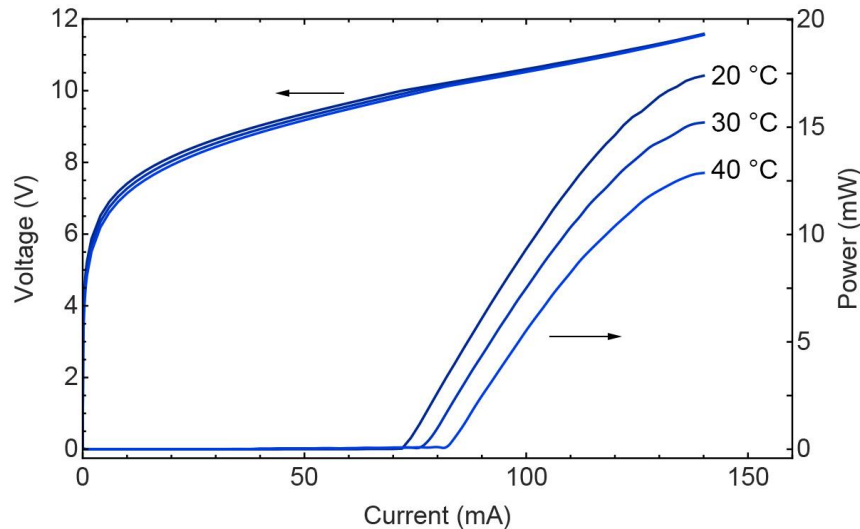
Processed DFB QC lasers





# DFB QC laser performance: 4.8 $\mu\text{m}$ wavelength for OCS detection

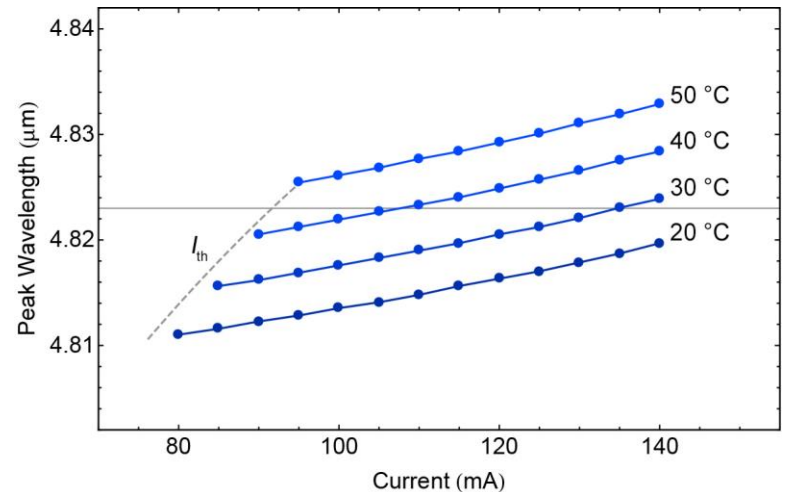
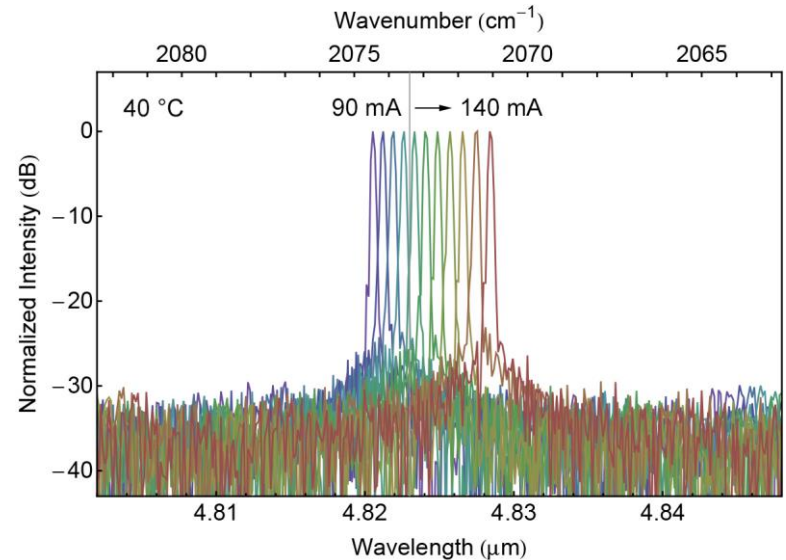
CW performance: 1 mm cavity, HR-coated back facet



Stable, single-mode emission with 750 mW  
CW threshold power consumption at 20 ° C

Mode-hop-free tuning across target  
wavelength above room temperature

Devices have been run for as long at 2000  
hours without degradation

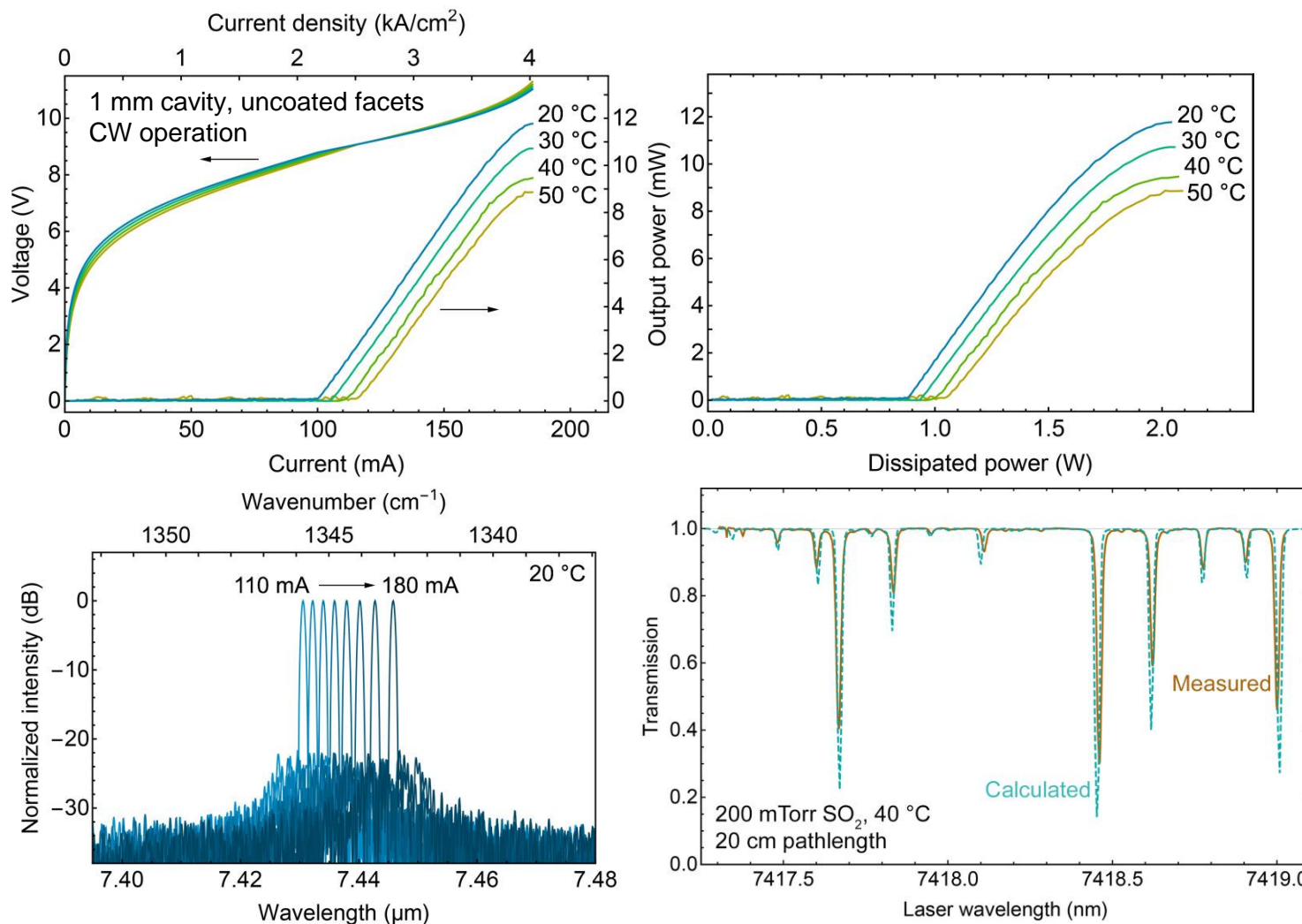


Briggs, et al., *Appl. Phys. Lett.* **105**, 141117 (2014)



Jet Propulsion Laboratory  
California Institute of Technology

# DFB QC laser performance: 7.4 $\mu\text{m}$ wavelength for $\text{SO}_2$ detection



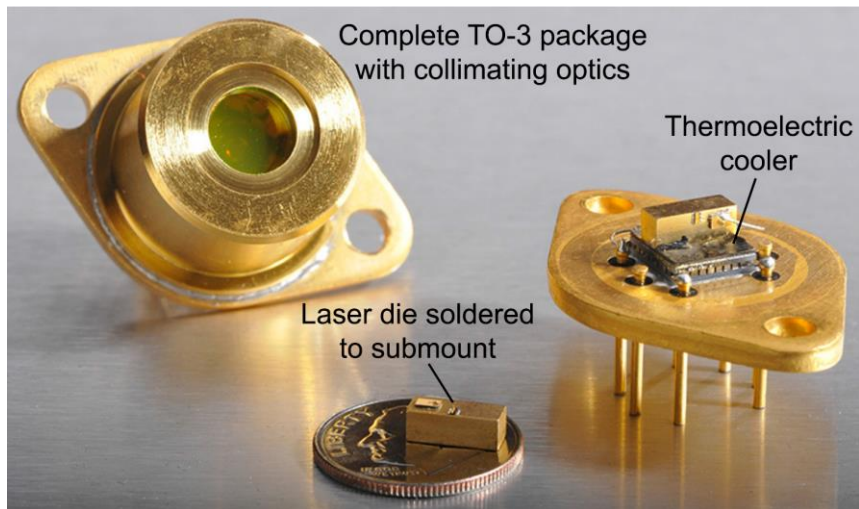
Briggs, et al., *Opt. Express* **24**, 14589 (2016)



Jet Propulsion Laboratory  
California Institute of Technology

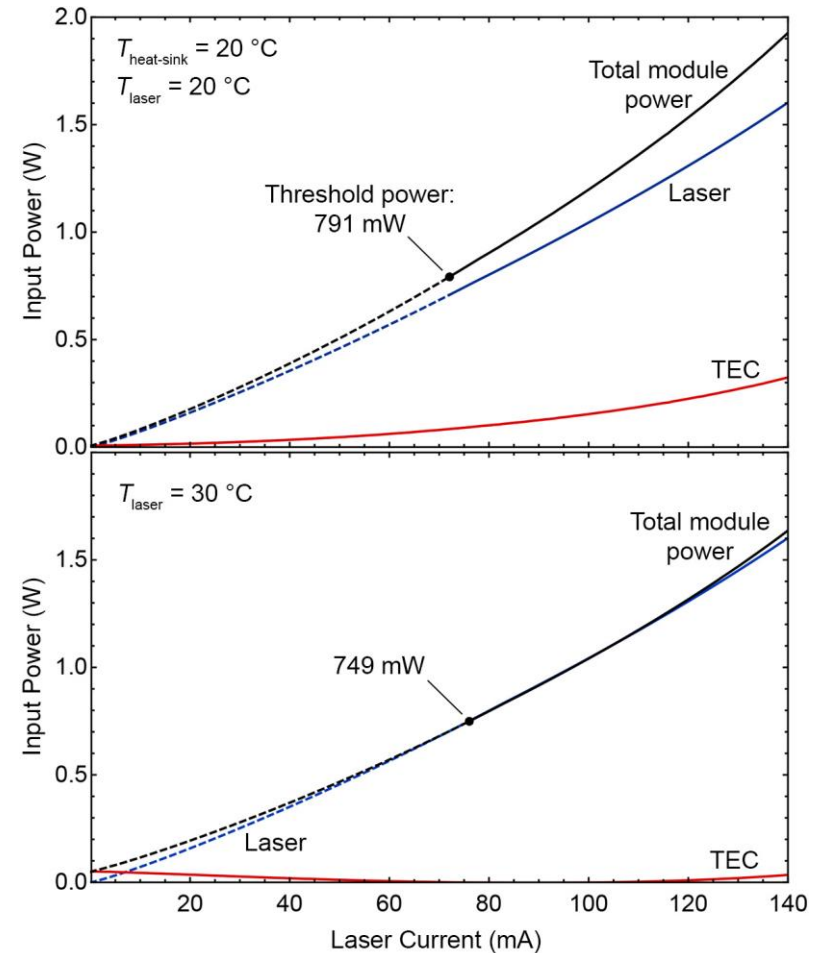
# QC laser packaging

## Packaged 4.8 $\mu\text{m}$ QC laser CW power consumption

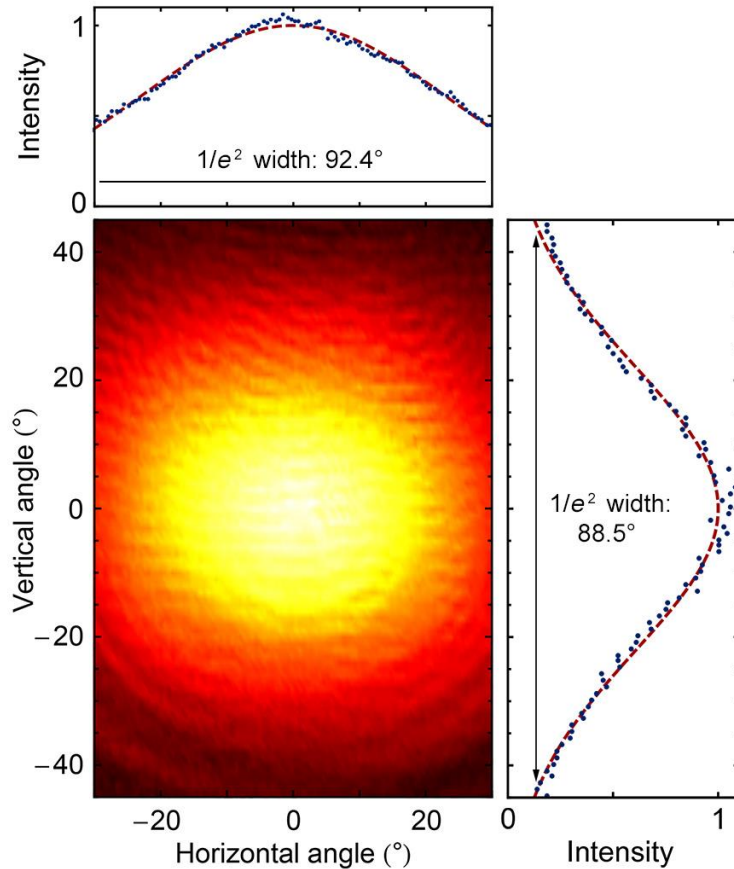


Low dissipation and high operating temperatures enable use of small form factor packages

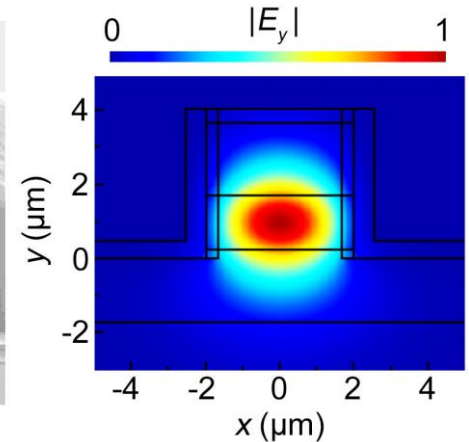
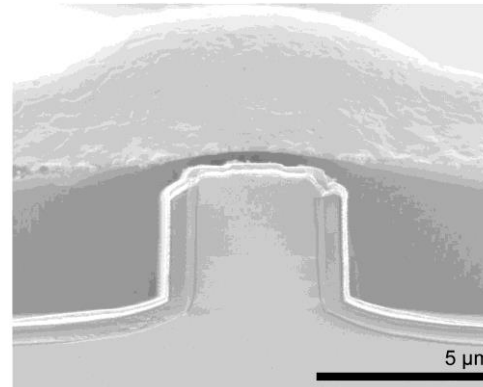
Demonstrated modules with power consumption <1 W at threshold and <2 W at maximum output



# Symmetric QC laser far-field profile



Measured far-field profile at 4.8 μm



Briggs, et al., *Appl. Phys. Lett.* **105**, 141117 (2014)

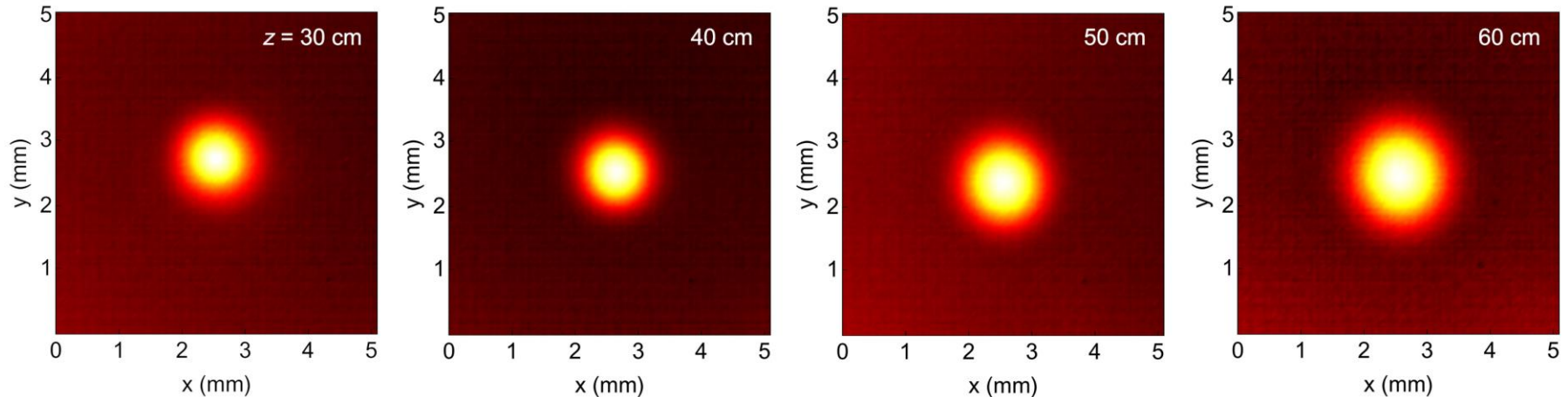
Low-index lateral cladding compensates for the asymmetric active region, resulting in a radially symmetric far-field profile

Enables efficient coupling to external optics

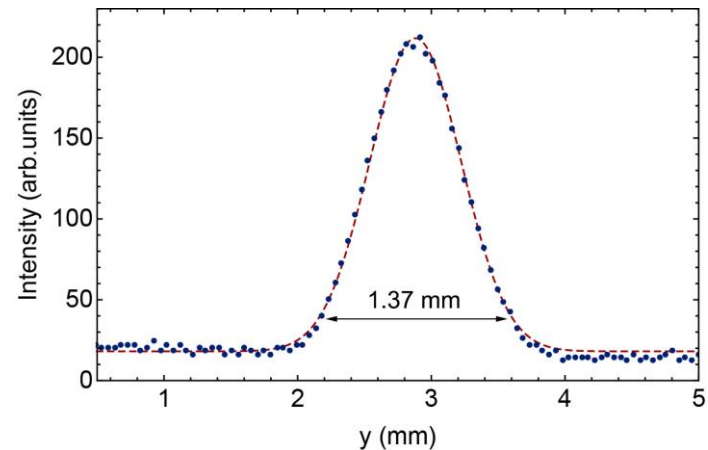
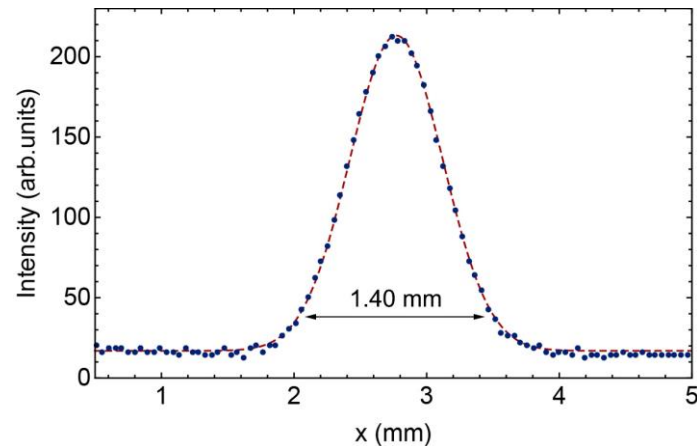


# Beam profiles for 7.4 $\mu\text{m}$ QC laser: Single aspheric collimating lens

Infrared camera images at varying distance,  $z$ , from the lens



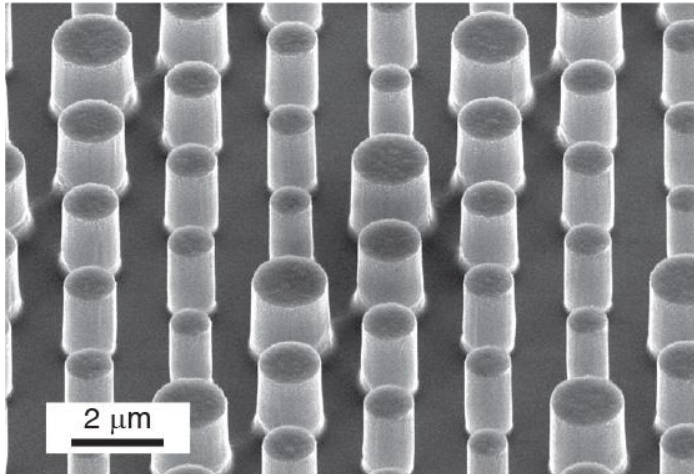
Horizontal and vertical beam profiles at  $z = 40\text{ cm}$



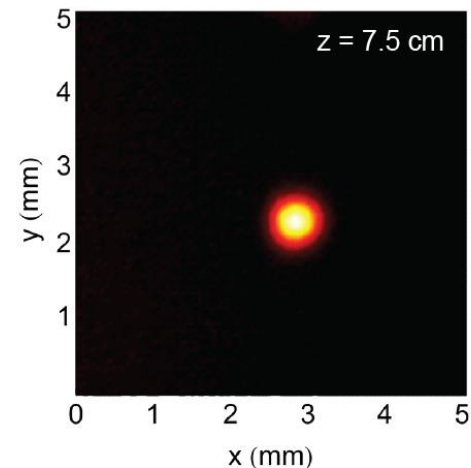
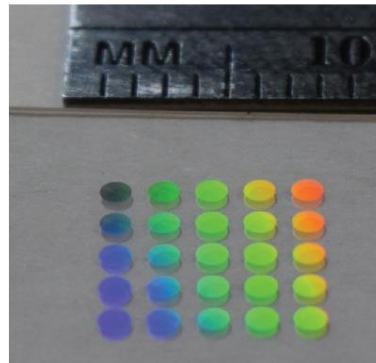
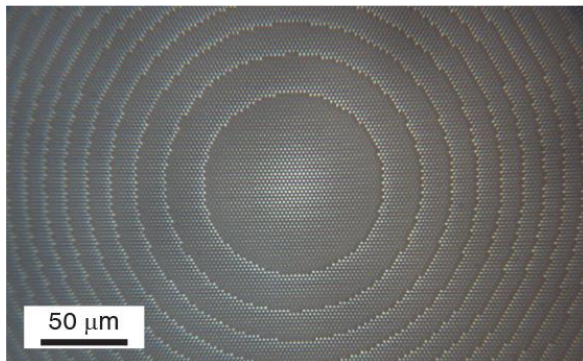
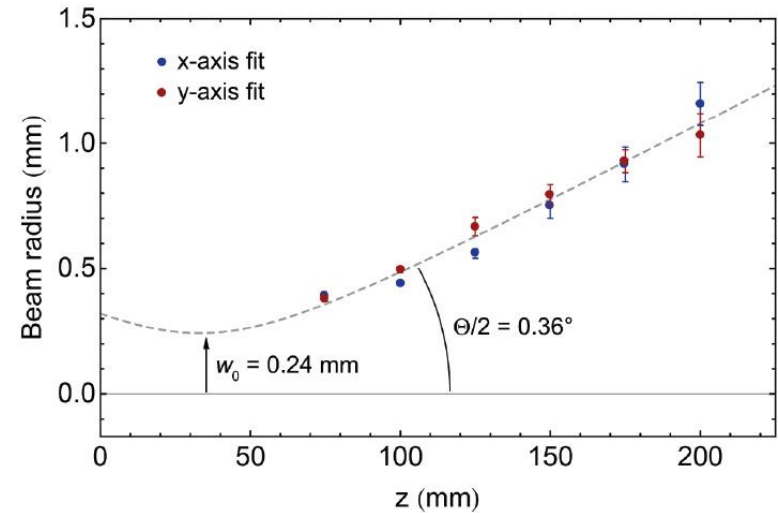


# Collimation using flat metasurface lenses

Flat lenses designed for 4.8  $\mu\text{m}$  QC laser collimation



Achieved collimation with  $M^2 = 1.02$

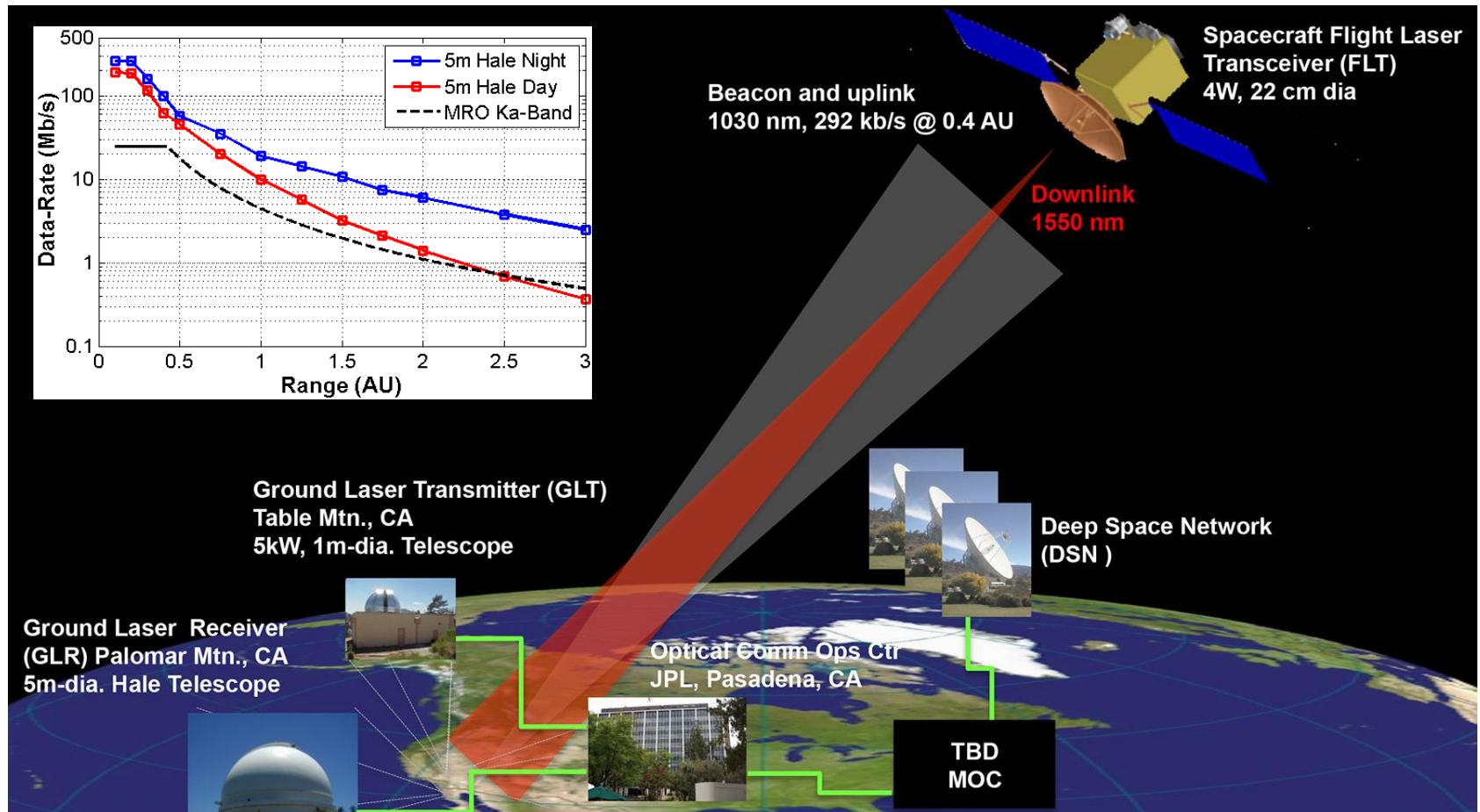


Arabi, et al., *Opt. Express* **23**, 33310 (2015)



Jet Propulsion Laboratory  
California Institute of Technology

# Deep space optical communication with SNSPD ground receivers

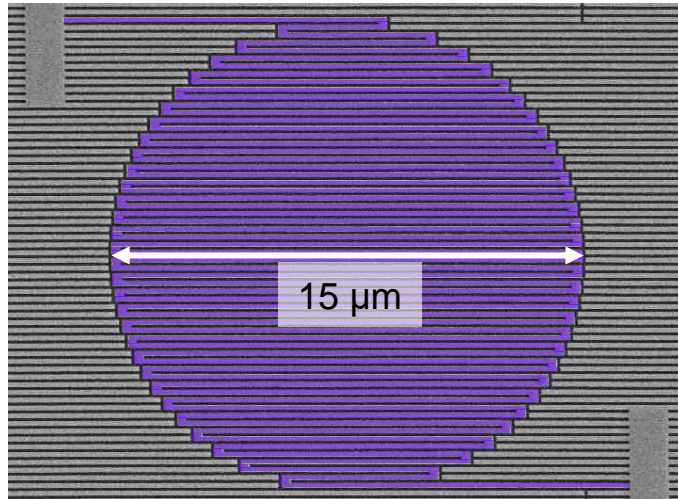


Ground receiver requires an efficient, photon-counting detector at 1550 nm

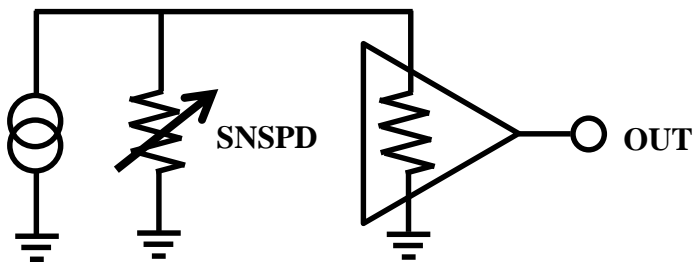


# SNSPD principle of operation

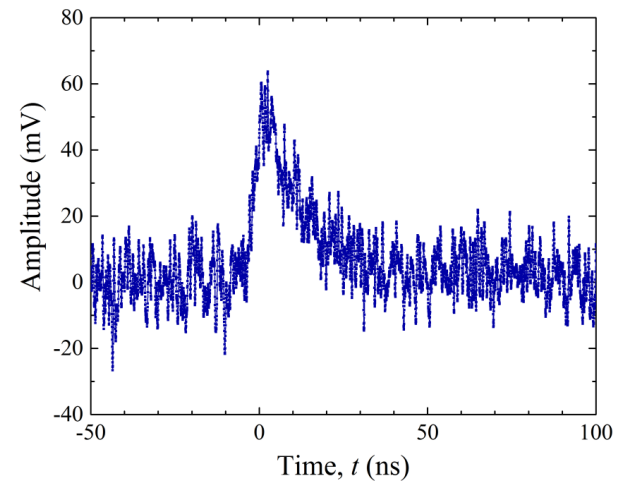
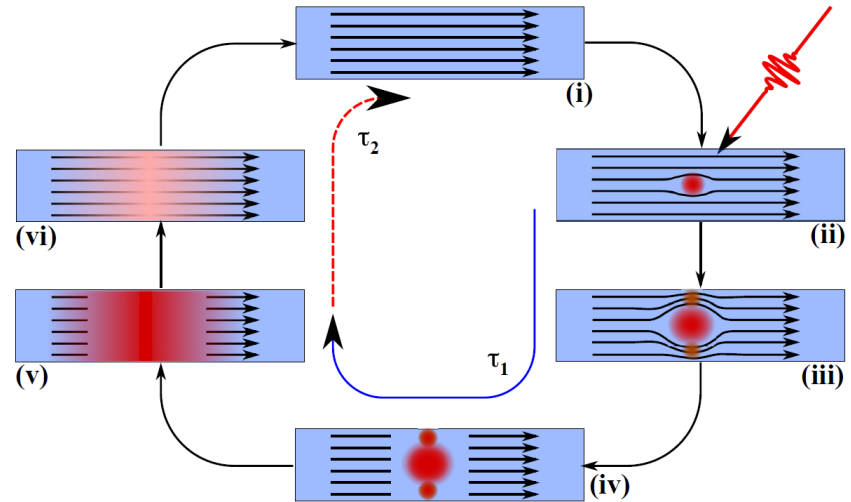
WSi-based single-nanowire detector



Readout concept

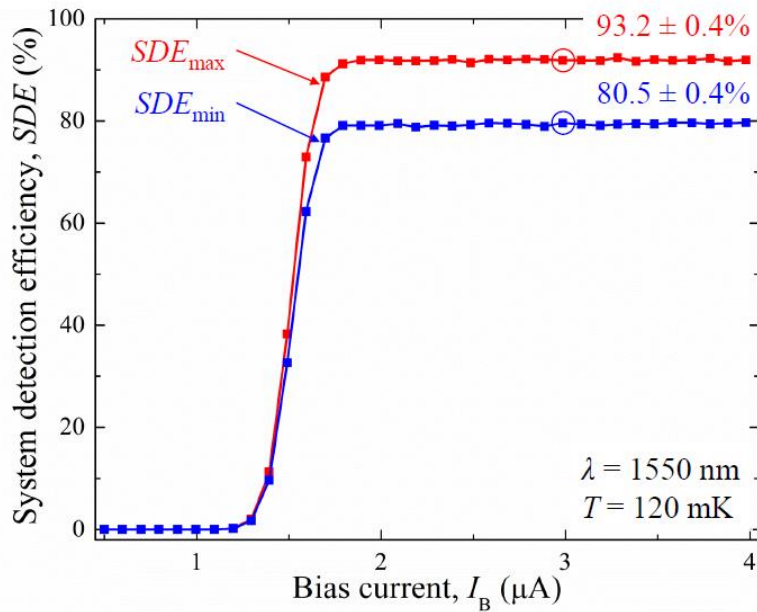


SNSPD detection process

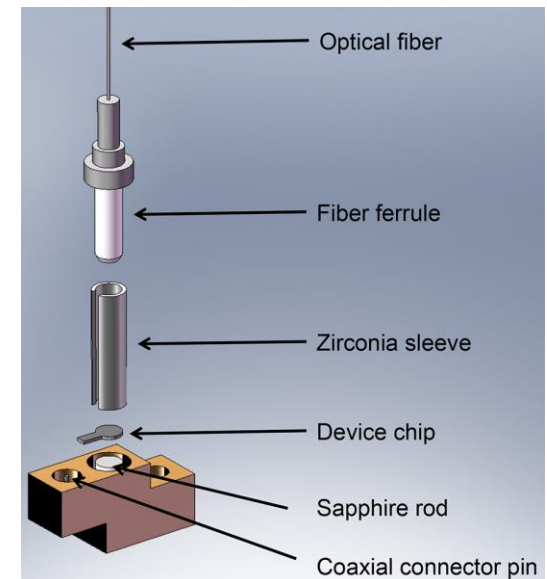
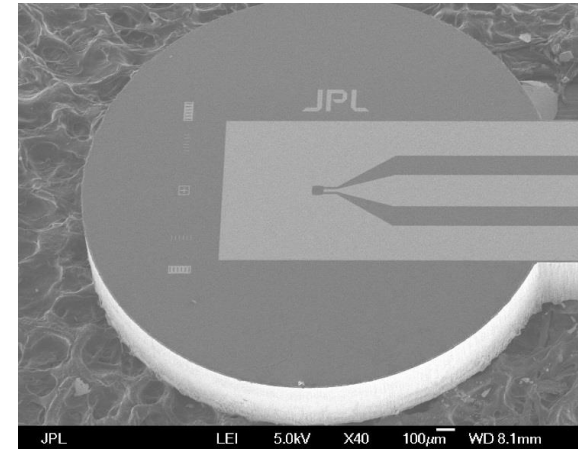


# High-efficiency single-pixel SNSPDs

WSi-based single-pixel, fiber-coupled detectors  
(in collaboration with S.W. Nam, *et al.*, NIST)



Marsili, *et al.*, *Nature Photon.* **7**, 210 (2013)



Miller, *et al.*, *Opt. Express* **19**, 9102 (2011)





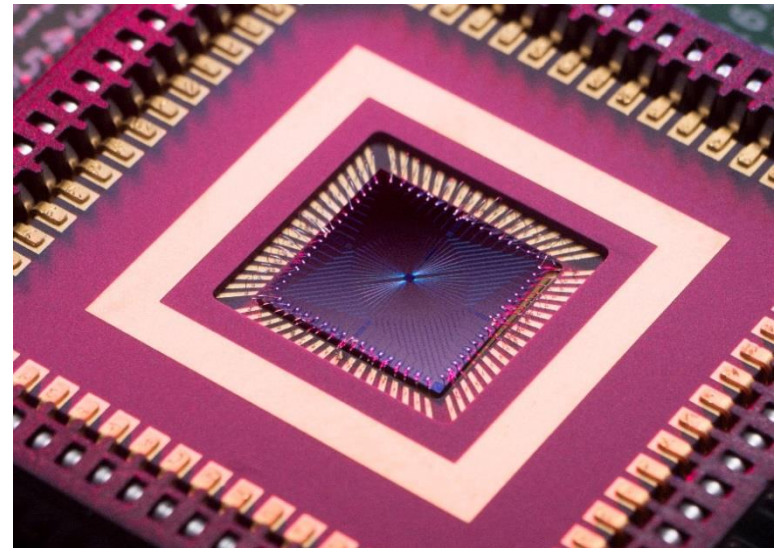
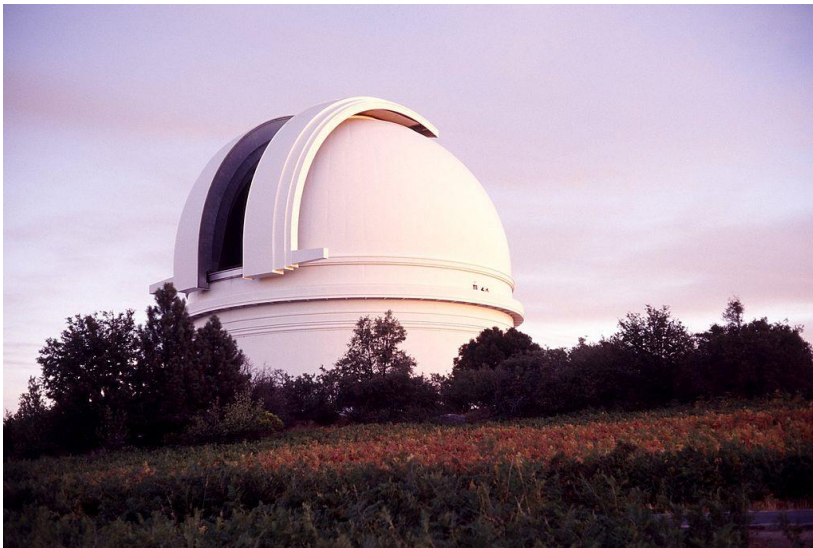
# Deep Space Optical Communication (DSOC) project

Kicking off now as a NASA Technology Demonstration Mission

Planned to launch with Discovery spacecraft in 2021

Goal is to transmit 264 Mbps from 0.16 AU, 45 kbps from 2.6 AU

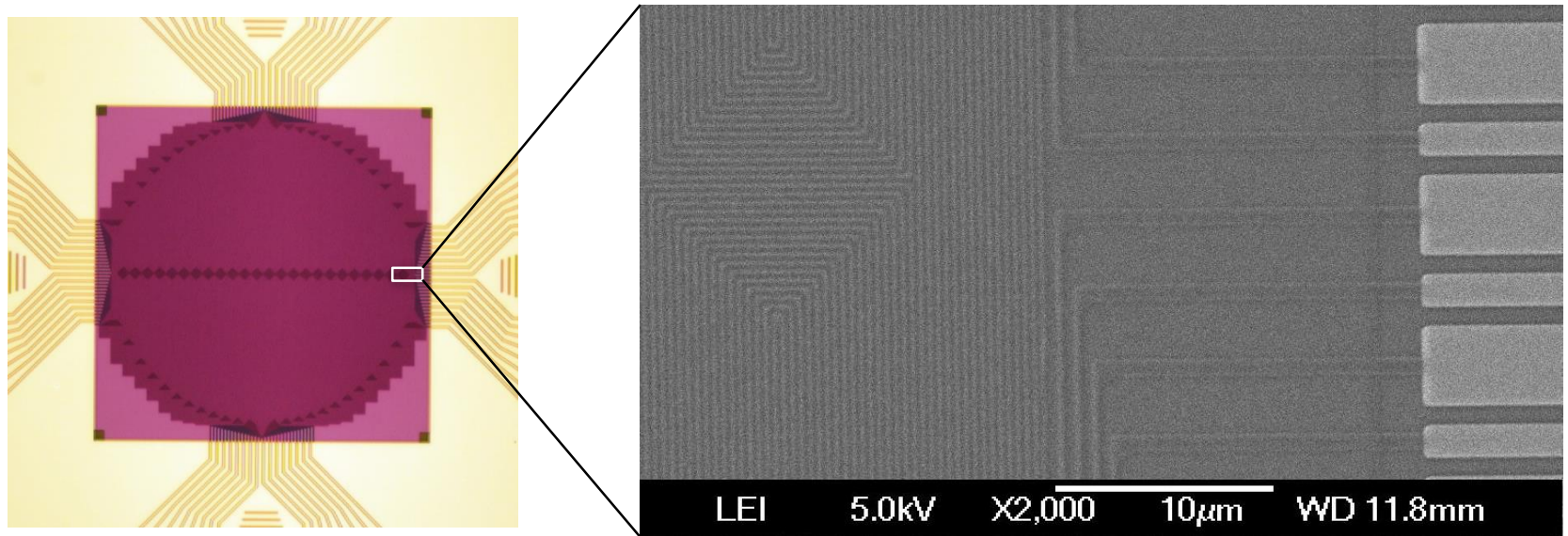
Ground terminal at the 5 m Palomar Hale telescope to use a 64-pixel WSi SNSPD array



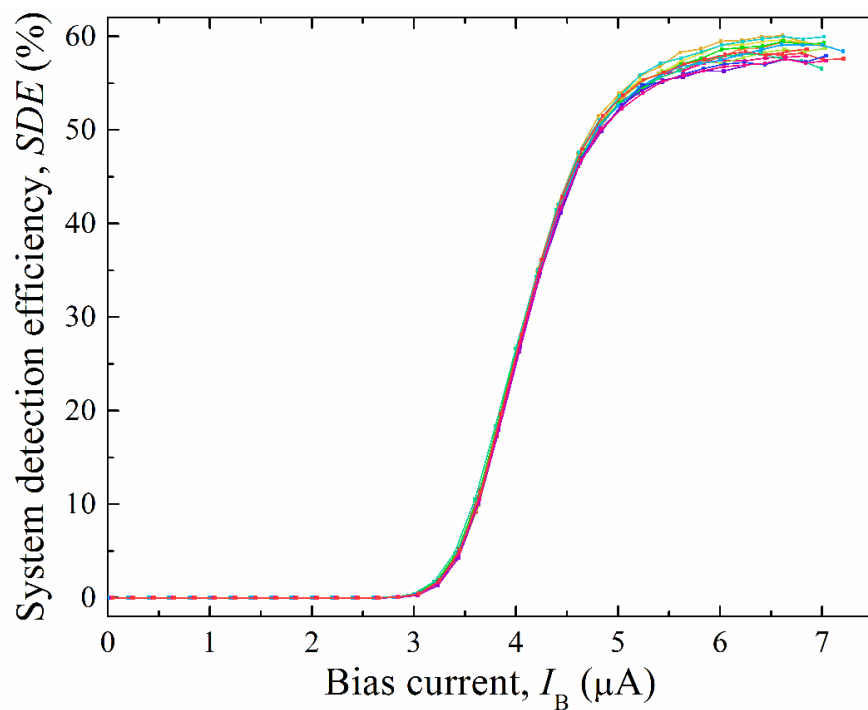


## High-count-rate SNSPD arrays

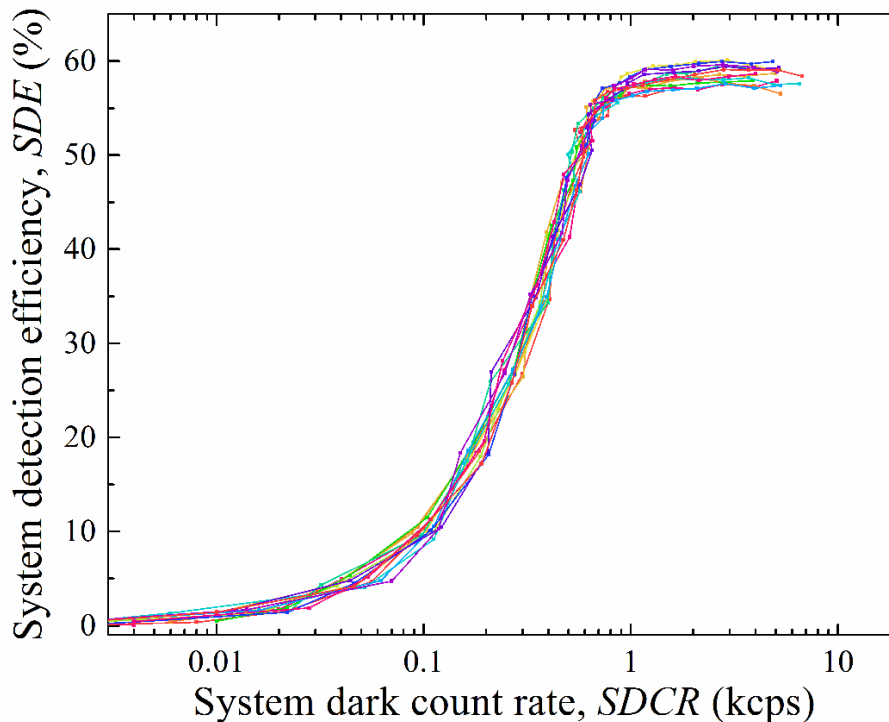
64-pixel SNSPD array with buried reflector and topside coating optimized for 1550 nm  
320- $\mu\text{m}$  diameter free-space coupled active area, 4 quadrants, 16 wires per quadrant  
10% nanowire fill factor: 4.5 x 160 nm wires on a 1.6  $\mu\text{m}$  pitch



## 64-pixel SNSPD array performance



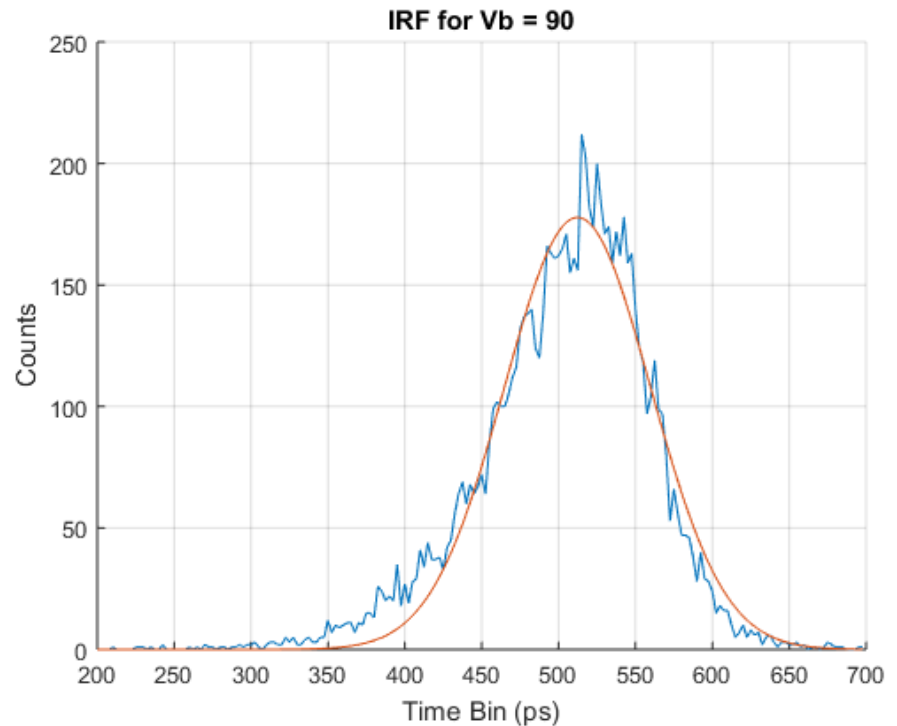
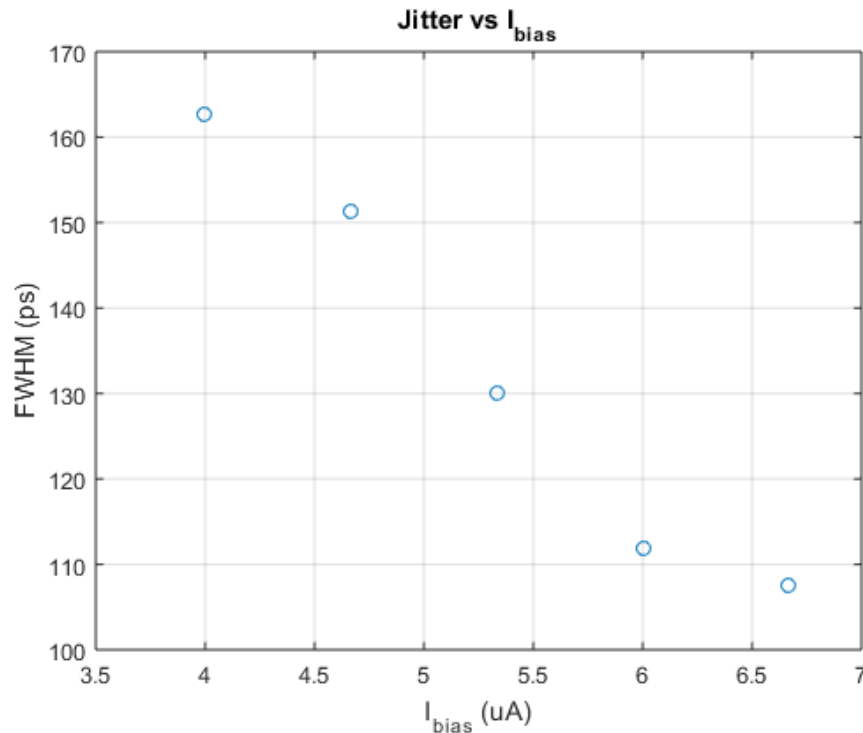
Measured 55% efficiency for 31 of 32 wires  
1.3 Gcps (assuming 60 active pixels)



<7 kcps dark count rate per pixel at  
maximum detection efficiency



## 64-pixel SNSPD array performance



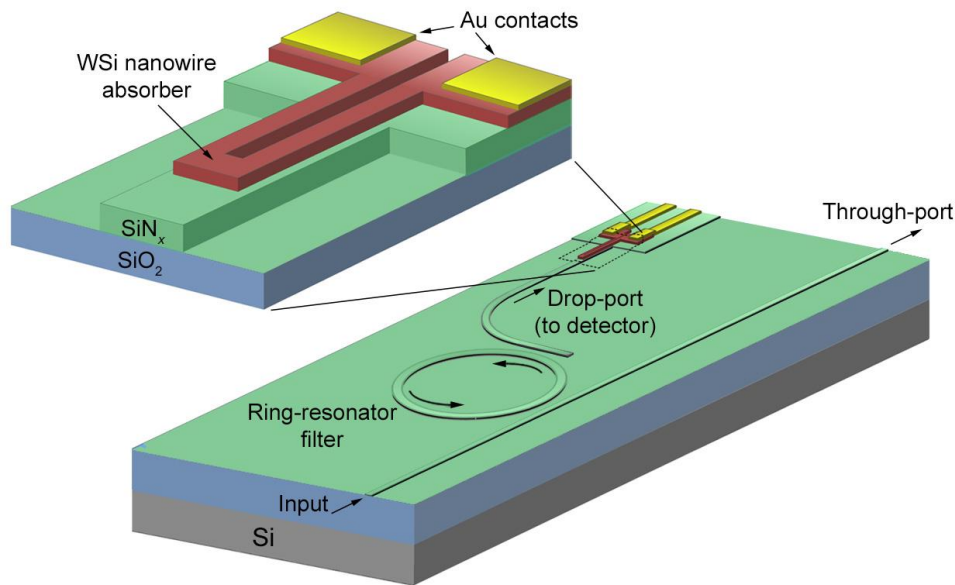
Measured timing jitter of <170 ps FWHM across detector bias plateau

Bias scaling suggests that readout noise is the dominant jitter mechanism

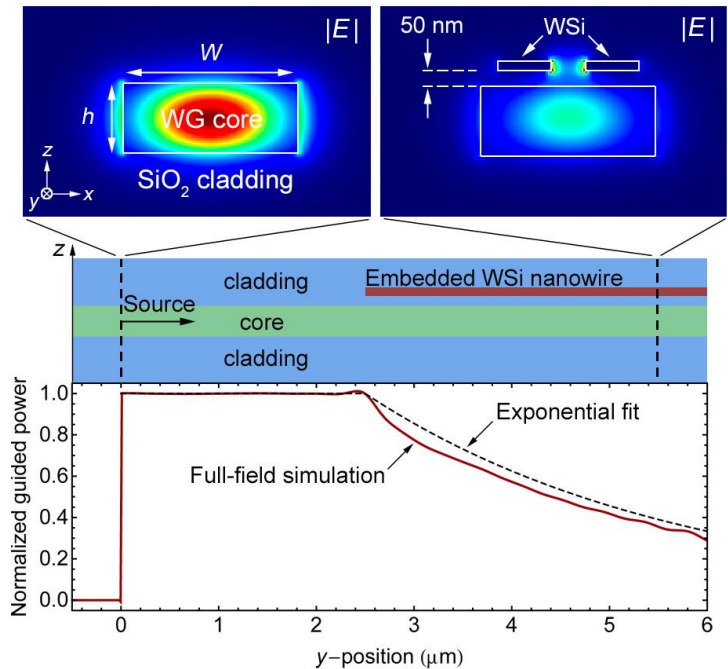


# Waveguide-integrated SNSPDs

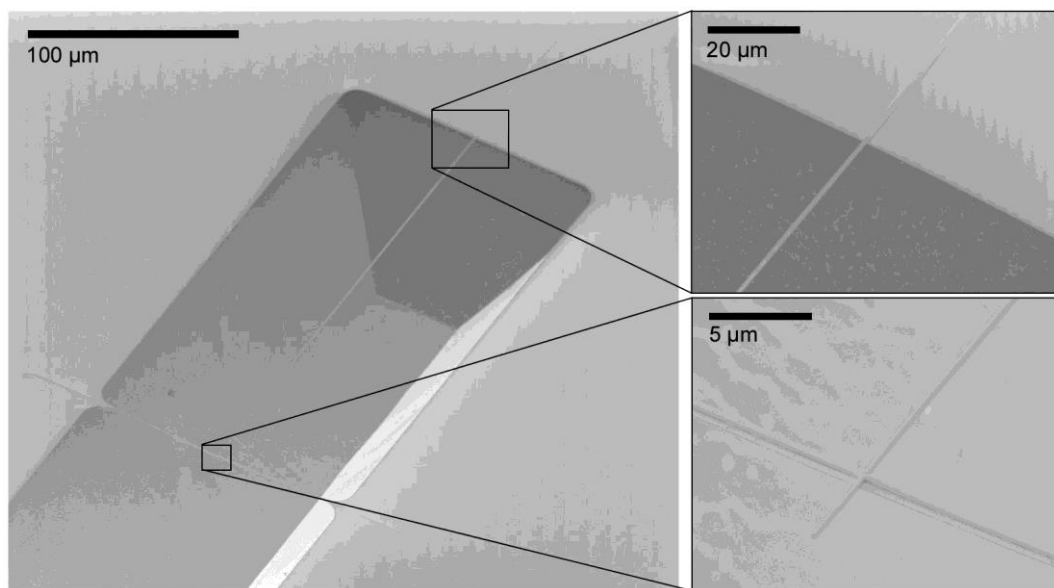
Single 5-nm-thick WSi hairpin patterned on top of a single-mode low-stress  $\text{SiN}_x$  waveguide



FDTD simulations indicate an expected absorption length of  $<10\ \mu\text{m}$  for the fundamental TE mode



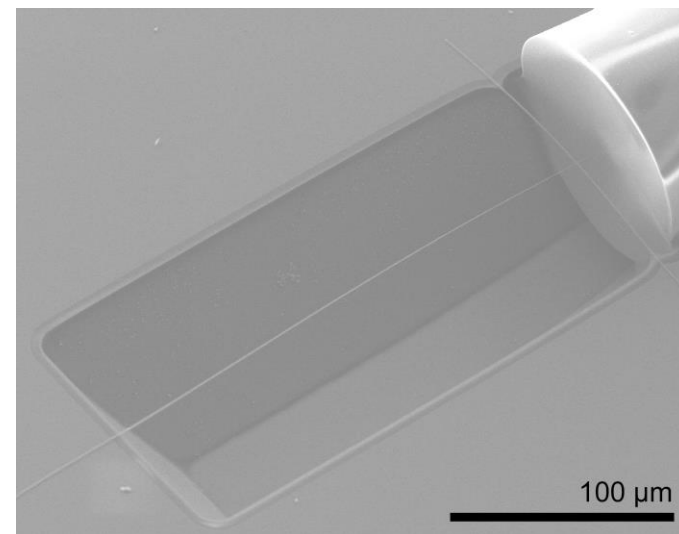
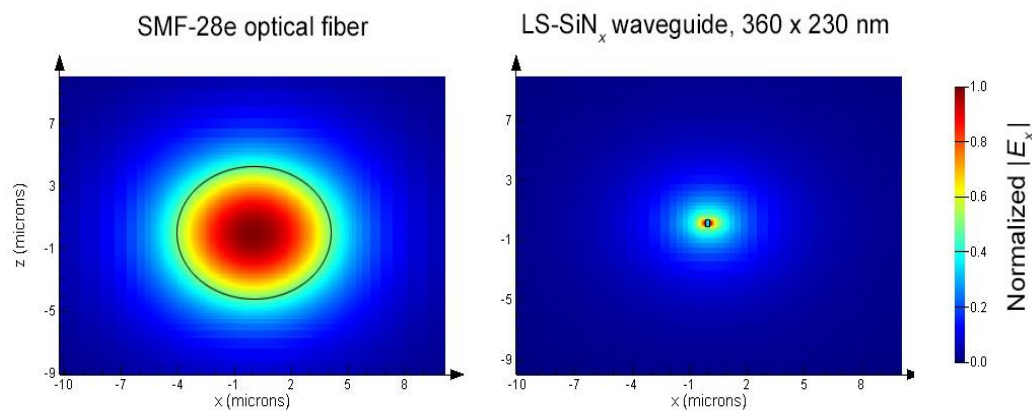
# Cryo-compatible suspended inverse-taper fiber couplers



Suspended low-stress  $\text{SiN}_x$  undercut by wet chemical etching

Mode-matching to standard fiber indicates calculated 86% coupling efficiency

Additional scattering from tether and substrate interface reduces calculated efficiency to 42%

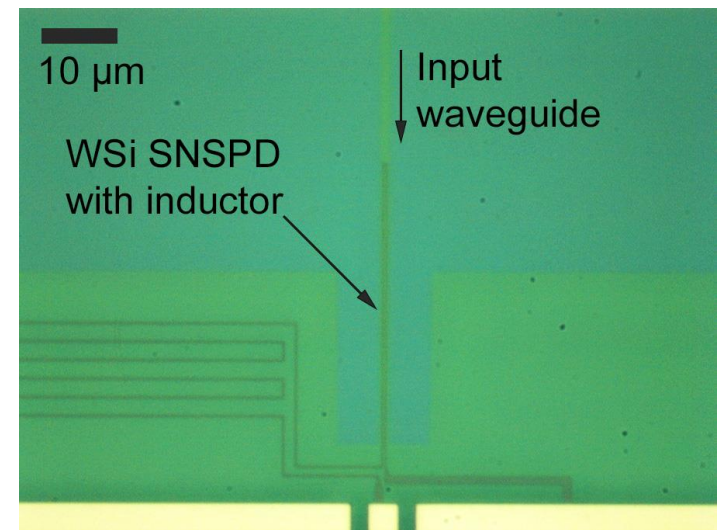
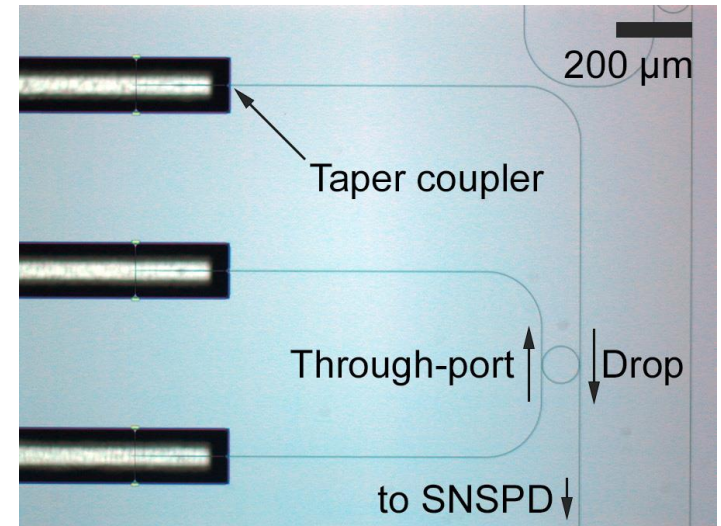
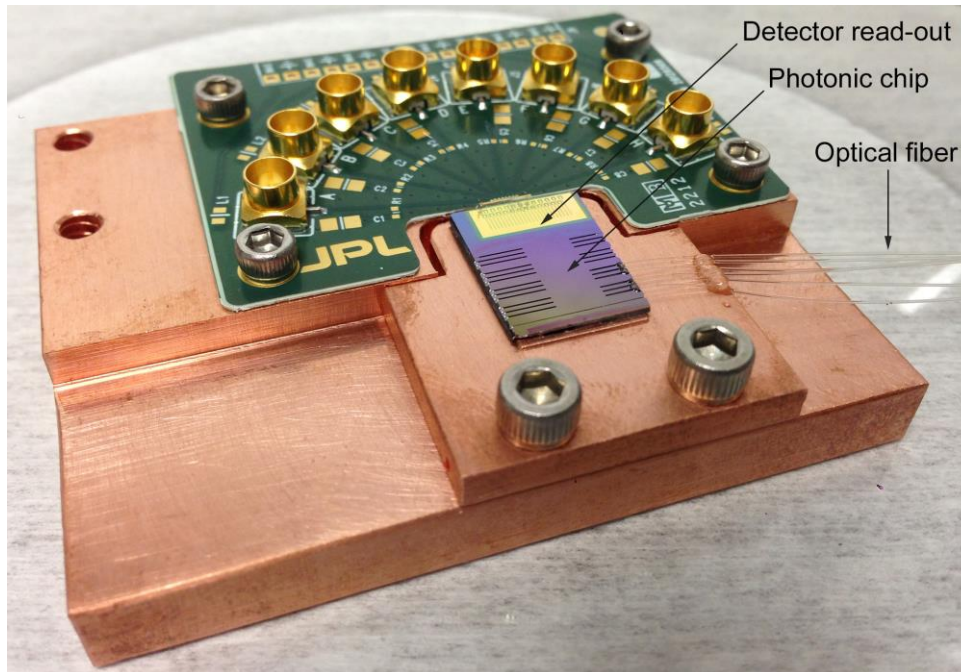




# Complete WG-SNSPD photonic chip

Three nominally identical fiber ports per SNSPD and eight SNSPDs per chip

Enables independent characterization of waveguide loss and detector performance

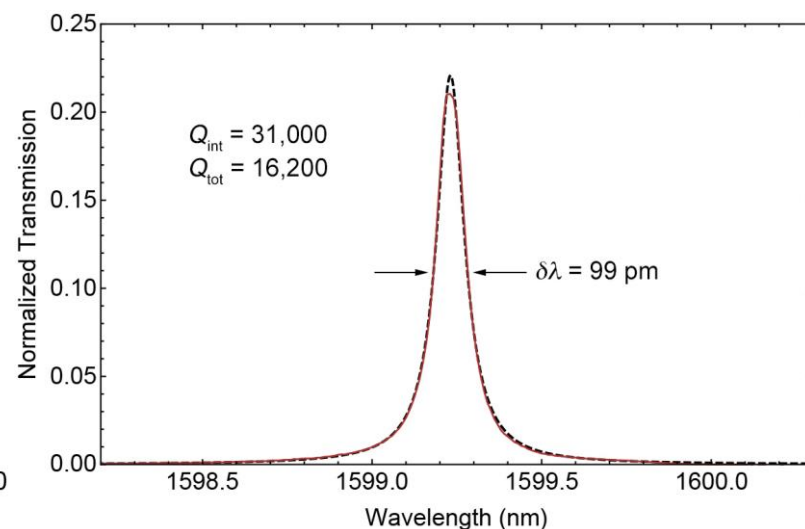
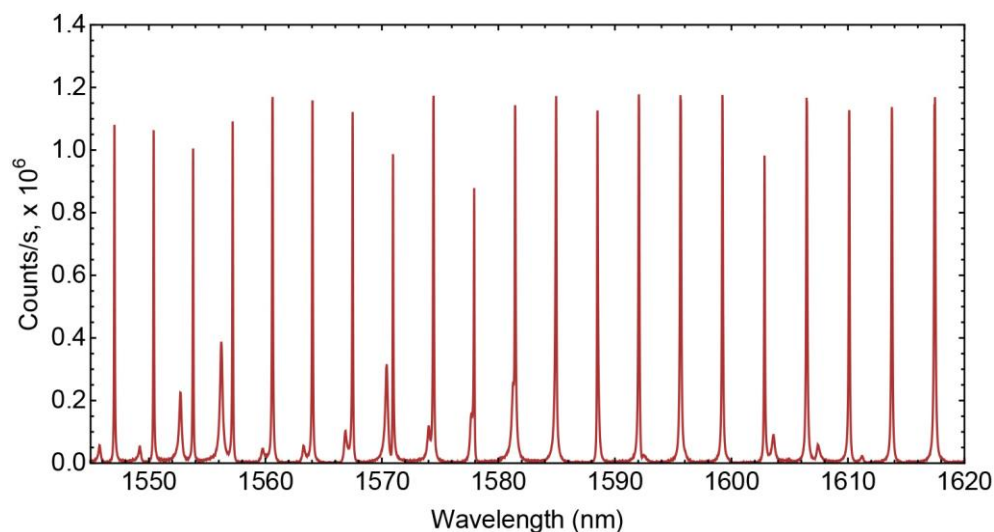


## Count rate vs. wavelength

Detector measurements show spectral filtering using a SNSPD coupled to a ring-resonator drop-port

FSR equivalent to conventional detector measurements, confirming TE mode operation

Weaker (more dispersive) resonances likely related to TM mode

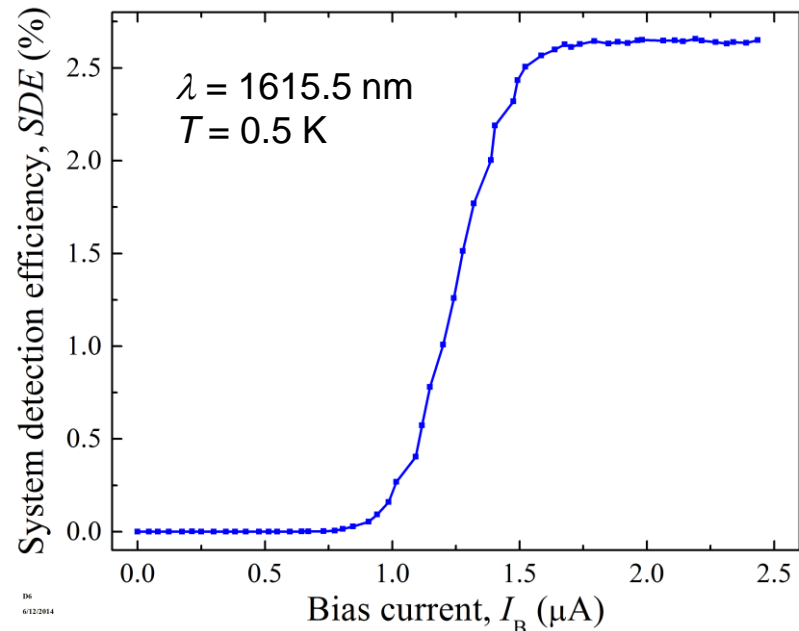
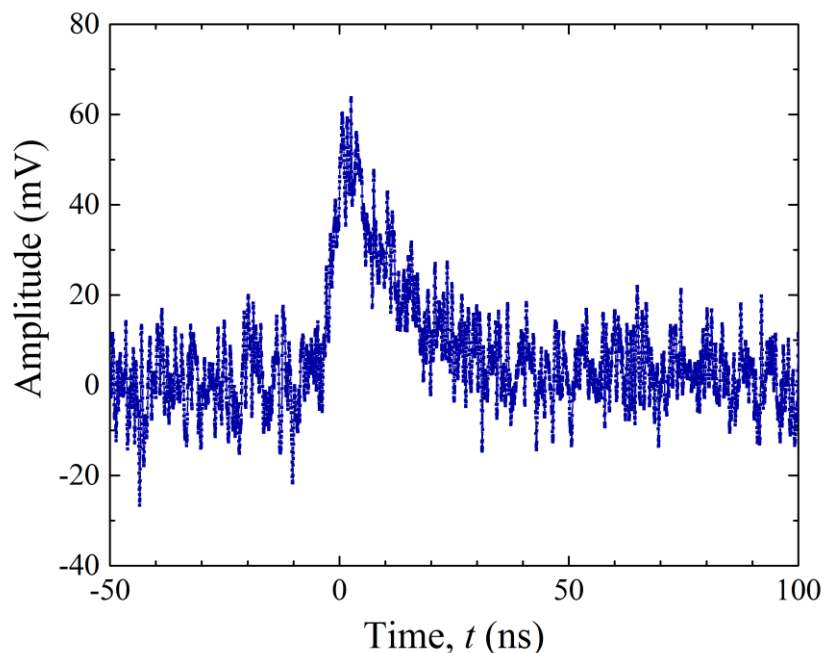


## Waveguide-integrated SNSPD performance

Detector pulses show recovery time of  $\sim 10$  ns

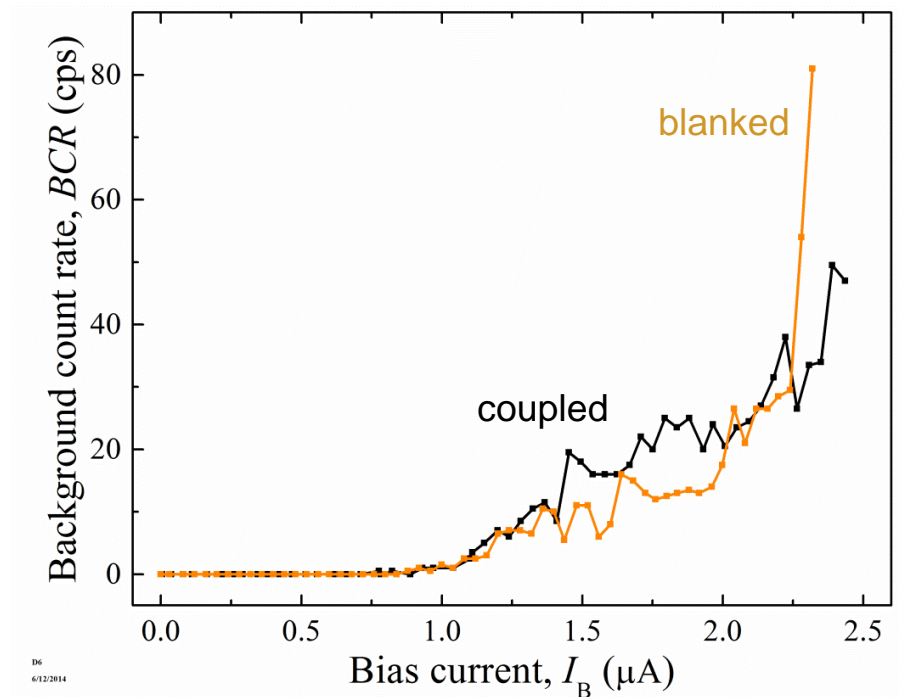
Saturation of counts with bias current indicates high internal efficiency

System detection efficiency limited by couplers and waveguide propagation loss



## Waveguide-integrated SNSPD dark counts

Low measured dark counts with and without fiber feed-through connected



---

# Acknowledgements

## **QC Lasers:**

### **- Coworkers:**

Clifford Frez, Mathieu Fradet, Mahmood Bagheri, Siamak Forouhar, and Chris Webster, *JPL*  
Christian Pflügl, Romain Blanchard, and Laurent Diehl, *Pendar Technologies*

### **- Project support:**

NASA Planetary Instrument Concepts and Solar System Observations (PICASSO) Program  
NASA New Frontiers Homesteader Program

## **SNSPDs:**

### **- Coworkers:**

Matthew Shaw, Andrew Beyer, Francesco Marsili, Jason Allmaras, and Bill Farr, *JPL*

### **- Project support:**

NASA Game Changing Development Program  
JPL Research And Technology Development Program

